



**HAL**  
open science

## Optimal Maturation of the SIV-Specific CD8<sup>+</sup> T Cell Response after Primary Infection Is Associated with Natural Control of SIV: ANRS SIC Study

Caroline Passaes, Antoine Millet, Vincent Madelain, Valérie Monceaux, Annie David, Pierre Versmisse, Naya Sylla, Emma Gostick, Sian Llewellyn-Lacey, David Price, et al.

### ► To cite this version:

Caroline Passaes, Antoine Millet, Vincent Madelain, Valérie Monceaux, Annie David, et al.. Optimal Maturation of the SIV-Specific CD8<sup>+</sup> T Cell Response after Primary Infection Is Associated with Natural Control of SIV: ANRS SIC Study. *Cell Reports*, 2020, 32 (12), pp.108174 -. 10.1016/j.celrep.2020.108174 . hal-03599642

**HAL Id: hal-03599642**

**<https://hal.science/hal-03599642>**

Submitted on 23 Sep 2022

**HAL** is a multi-disciplinary open access archive for the deposit and dissemination of scientific research documents, whether they are published or not. The documents may come from teaching and research institutions in France or abroad, or from public or private research centers.

L'archive ouverte pluridisciplinaire **HAL**, est destinée au dépôt et à la diffusion de documents scientifiques de niveau recherche, publiés ou non, émanant des établissements d'enseignement et de recherche français ou étrangers, des laboratoires publics ou privés.



Distributed under a Creative Commons Attribution - NonCommercial 4.0 International License

1 **Optimal maturation of the SIV-specific CD8<sup>+</sup> T-cell response after primary infection**  
2 **is associated with natural control of SIV. ANRS SIC study**

3  
4 Caroline Passaes<sup>1,2</sup>, Antoine Millet<sup>3</sup>, Vincent Madelain<sup>4</sup>, Valérie Monceaux<sup>1</sup>, Annie David<sup>1</sup>,  
5 Pierre Versmisse<sup>1</sup>, Naya Sylla<sup>2</sup>, Emma Gostick<sup>5</sup>, Sian Llewellyn-Lacey<sup>5</sup>, David A. Price<sup>5</sup>,  
6 Antoine Blancher<sup>6,7</sup>, Nathalie Dereuddre-Bosquet<sup>2</sup>, Delphine Desjardins<sup>2</sup>, Gianfranco  
7 Pancino<sup>1</sup>, Roger Le Grand<sup>2</sup>, Olivier Lambotte<sup>2,8</sup>, Michaela Müller-Trutwin<sup>1</sup>, Christine  
8 Rouzioux<sup>3,9</sup>, Jeremie Guedj<sup>4</sup>, Veronique Avettand-Fenoel<sup>3,9</sup>, Bruno Vaslin<sup>2,#</sup>, Asier Sáez-  
9 Ciri6n<sup>1,#,\*</sup>

10

11 <sup>1</sup> Institut Pasteur, HIV Inflammation and Persistence, Paris, France.

12 <sup>2</sup> CEA – Universit6 Paris-Saclay, INSERM UMR1184, Immunology of Viral Infections and Autoimmune Diseases,  
13 IDMIT Department, IBFJ, Fontenay-aux-Roses, France.

14 <sup>3</sup> Universit6 Paris-Descartes, Sorbonne Paris Cit6, Facult6 de M6decine, EA 7327, Paris, France.

15 <sup>4</sup> Universit6 Paris-Diderot, IAME, INSERM UMR 1137, Sorbonne Paris Cit6, Paris, France.

16 <sup>5</sup> Cardiff University School of Medicine, Division of Infection and Immunity, Cardiff, UK.

17 <sup>6</sup> Universit6 Paul Sabatier, Laboratoire d'Immunog6n6tique Mol6culaire, EA 3034, Toulouse, France.

18 <sup>7</sup> CHU de Toulouse, Laboratoire d'Immunologie, Toulouse, France.

19 <sup>8</sup> Assistance Publique-H6pitaux de Paris, Service de M6decine Interne et Immunologie Clinique, Groupe  
20 Hospitalier Universit6 Paris-Saclay, H6pital Bic6tre, Le Kremlin-Bic6tre, France.

21 <sup>9</sup> Assistance Publique-H6pitaux de Paris, Service de Microbiologie Clinique, H6pital Necker-Enfants Malades,  
22 Paris, France.

23

24 #These authors contributed equally to this work.

25 \*Lead contact

26 Correspondence to: [bruno.vaslin@cea.fr](mailto:bruno.vaslin@cea.fr) or [asier.saez-cirion@pasteur.fr](mailto:asier.saez-cirion@pasteur.fr)

27

28 **ABSTRACT**

29 Highly efficient CD8<sup>+</sup> T-cells are associated with natural HIV control, but it has remained  
30 unclear how these cells are generated and maintained. We have used a macaque model of  
31 spontaneous SIVmac251 control to monitor the development of efficient CD8<sup>+</sup> T-cell  
32 responses. SIV-specific CD8<sup>+</sup> T-cells emerge during primary infection in all animals. The  
33 ability of CD8<sup>+</sup> T-cells to suppress SIV is suboptimal in the acute phase but increases  
34 progressively in controller macaques before the establishment of sustained low-level  
35 viremia. Controller macaques develop optimal memory-like SIV-specific CD8<sup>+</sup> T-cells early  
36 after infection. In contrast, a persistently skewed differentiation phenotype is observed  
37 among memory SIV-specific CD8<sup>+</sup> T-cells in non-controller macaques. The phenotype of SIV-  
38 specific CD8<sup>+</sup> T-cells defined early after infection appears to favor the development of  
39 protective immunity in controllers, whereas SIV-specific CD8<sup>+</sup> T-cells in non-controllers fail to  
40 gain antiviral potency, feasibly as a consequence of early defects imprinted in the memory  
41 pool.

## 42 INTRODUCTION

43 The ability of CD8<sup>+</sup> T-cells to control viral replication has been extensively documented in the  
44 setting of HIV/SIV infection (McBrien et al., 2018; Walker and McMichael, 2012). Primary  
45 infection is characterized by massive viremia, which subsides following the expansion of  
46 HIV/SIV-specific CD8<sup>+</sup> T-cells (Borrow et al., 1994; Koup et al., 1994). However, the virus is  
47 not eradicated, leading to the emergence of immune escape variants (Allen et al., 2000;  
48 Borrow et al., 1997; O'Connor et al., 2002; Price et al., 1997) and ongoing antigen exposure,  
49 which drives CD8<sup>+</sup> T-cell exhaustion during the chronic phase of infection (Day et al., 2006;  
50 Petrovas et al., 2006; Petrovas et al., 2007; Trautmann et al., 2006). These observations  
51 suggest that naturally generated HIV/SIV-specific CD8<sup>+</sup> T-cells are frequently suboptimal in  
52 terms of antiviral efficacy, potentially reflecting limited cross-reactivity and/or intrinsic  
53 defects in the arsenal of effector functions required to eliminate infected CD4<sup>+</sup> T-cells (Du et  
54 al., 2016; Lecuroux et al., 2013). The latter possibility is especially intriguing in light of *ex vivo*  
55 experiments showing that effective suppression of viral replication is a particular feature of  
56 CD8<sup>+</sup> T-cells isolated from HIV controllers (HICs) (Angin et al., 2016; Saez-Cirion et al., 2007;  
57 Saez-Cirion et al., 2009; Tansiri et al., 2015).

58

59 HICs are a rare group of individuals who control viremia to very low levels without  
60 antiretroviral therapy (Saez-Cirion and Pancino, 2013). Understanding the mechanisms  
61 associated with such spontaneous control of HIV infection seems crucial for the  
62 development of new strategies designed to achieve remission. Efficient CD8<sup>+</sup> T-cell  
63 responses are almost universally present in HICs (Betts et al., 2006; Chowdhury et al., 2015;  
64 Hersperger et al., 2011a; Hersperger et al., 2010; Migueles et al., 2002; Migueles et al., 2008;  
65 Saez-Cirion et al., 2007; Saez-Cirion et al., 2009; Zimmerli et al., 2005). These individuals also

66 frequently express the protective human leukocyte antigen (HLA) class I allotypes HLA-B\*27  
67 and HLA-B\*57, further supporting a key role for CD8<sup>+</sup> T-cells in the natural control of HIV  
68 (Lecuroux et al., 2014; Migueles et al., 2000; Pereyra et al., 2008). However, the presence of  
69 these allotypes is not sufficient to confer protection, and potent CD8<sup>+</sup> T-cell responses with  
70 the ability to suppress HIV replication directly *ex vivo* also occur in HICs expressing non-  
71 protective allotypes (Lecuroux et al., 2014). In addition, the qualitative properties of CD8<sup>+</sup> T-  
72 cells from HICs have only been characterized extensively during chronic infection, when  
73 viremia was already under control, often several years after the acquisition of HIV. It has  
74 therefore remained unclear how these high-quality CD8<sup>+</sup> T-cell responses develop from the  
75 early stages of infection and evolve over time.

76

77 *Cynomolgus* macaques (CyMs, *Macaca fascicularis*) infected with SIVmac251 closely  
78 recapitulate the dynamics and key features of HIV infection, including similar levels of viral  
79 replication in the acute and chronic phases of infection, memory CD4<sup>+</sup> T-cell depletion, rapid  
80 seeding of the viral reservoir, and eventual progression to AIDS (Antony and MacDonald,  
81 2015; Feichtinger et al., 1990; Karlsson et al., 2007; Mannioui et al., 2009; Putkonen et al.,  
82 1989). Moreover, some individuals control infection naturally, as in humans. CyMs from  
83 Mauritius offer the additional advantage of limited major histocompatibility complex (MHC)  
84 diversity, making them particularly attractive for the study of CD8<sup>+</sup> T-cell responses. Natural  
85 control of SIV in Mauritian CyMs is favored by the MHC haplotype M6 (Aarnink et al., 2011;  
86 Mee et al., 2009). Inoculation with low-dose SIV via the intrarectal (*i.r.*) route is also  
87 associated with natural control, irrespective of MHC haplotype (Bruel et al., 2015). We took  
88 advantage of these validated models to study the dynamics of SIV-specific CD8<sup>+</sup> T-cell  
89 responses in blood and tissues from the onset of infection in controllers and viremic CyMs.

90 Using this approach, we identified an optimal maturation pathway in SICs that enabled SIV-  
91 specific CD8<sup>+</sup> T-cells to acquire potent antiviral functions, which contributed to control  
92 infection.

93

94 **RESULTS**

95 ***SIV controllers are characterized by partial restoration of CD4<sup>+</sup> T-cell counts and***  
96 ***progressive decline in the frequency of SIV-infected cells in blood***

97 We monitored prospectively the outcome of infection in 12 SIV controllers (SICs) and 4  
98 viremic CyMs (VIRs) inoculated *i.r.* with SIVmac251. These animals carried or not the  
99 protective M6 haplotype and were inoculated with 5 or 50 animal infectious dose<sub>50</sub> (AID<sub>50</sub>) of  
100 SIVmac251 (Table S1). SIV controllers decreased plasma viral load (VL) to levels below 400  
101 SIV-RNA copies/mL, at least twice, over a follow up period of 18 months, while VIRs  
102 consistently maintained VL above 400 SIV-RNA copies/mL. The threshold of 400 RNA  
103 copies/mL was chosen in coherence with our studies in human cohorts of natural HIV control  
104 (Angin et al., 2016; Noel et al., 2016; Saez-Cirion et al., 2013; Saez-Cirion et al., 2007; Saez-  
105 Cirion et al., 2009). Ten SICs achieved control of viremia within 3 months. The other two SICs  
106 (BL669 and BO413) achieved VL below 400 SIV-RNA copies/mL for the first time 14 months  
107 after inoculation. One VIR (AV979) developed a tonsilar lymphoma, an AIDS related event  
108 reported at high frequency in this species upon SIV infection (Feichtinger et al., 1990).

109

110 Some differences in peak viremia were observed between SICs and VIRs (Figure 1A, Table  
111 S2). These differences became more pronounced over time (Figure 1A), because plasma  
112 viremia was suppressed more rapidly in SICs versus VIRs (Table S2). Levels of cell-associated  
113 SIV-DNA in blood from SICs and VIRs were comparable before peak viremia, but differences  
114 became apparent as plasma VLs declined and were maintained throughout chronic infection  
115 (Figure 1C, Table S2). Likewise, CD4<sup>+</sup> T-cells obtained during early infection from SICs and  
116 VIRs produced similar levels of p27 upon stimulation *ex vivo* with ConA and IL-2 (Figure S1A).  
117 However, while p27 production remained relatively stable in VIRs, these levels strongly

118 dropped overtime in SICs. We found a significant correlation between the levels of p27-  
119 production by CD4<sup>+</sup> T-cells and the levels of SIV-DNA ( $r=0.775$ ;  $p=0.0002$ , 6 months post-  
120 infection). Therefore, our results show that SICs, not only progressively reduced the  
121 frequency of total infected cells, but also the translation-competent reservoir. In addition,  
122 CD4<sup>+</sup> T-cell counts declined markedly in blood from both SICs and VIRs during primary  
123 infection (Figure 1B, Table S2). Subsequently, a degree of recovery was observed in SICs,  
124 whereas further gradual decline was observed in VIRs (Figure 1B, Table S2).

125

126 These results evidenced the distinctive dynamics of SIV infection in SICs and VIRs,  
127 characterized by very modest differences during the early weeks following inoculation that  
128 were progressively exacerbated during transition to chronic infection. The differences  
129 between SICs and VIRs during the chronic phase of SIV infection were consistent with the  
130 observations in human cohorts of HIV controllers.

131

### 132 ***SIV control is associated with early preservation of lymph nodes***

133 To characterize the extent of SIV control in greater depth, we monitored CD4<sup>+</sup> T-cells and  
134 total SIV-DNA longitudinally in peripheral lymph nodes (PLNs) and rectal biopsies (RBs). At  
135 the end of the study, we conducted similar evaluations in bone marrow, spleen, mesenteric  
136 lymph nodes (MLNs), and colonic mucosa, comparing SICs versus VIRs. The frequency of  
137 CD4<sup>+</sup> T-cells similarly declined in RBs from both SICs and VIRs during the acute stage of  
138 primary infection. While the frequency of CD4<sup>+</sup> T-cells was later partially restored in SICs, it  
139 continued to decline in VIRs (Figure 1D). These results matched the observations in blood  
140 samples (Figure 1B). In contrast, the frequency of CD4<sup>+</sup> T-cells was maintained close to  
141 baseline in PLNs from SICs, even during primary infection (day 14 post-infection [*p.i.*]), but

142 steadily declined over time in VIRs (Figure 1E). At the time of euthanasia, CD4<sup>+</sup> T-cell  
143 frequencies were substantially higher in blood (Figure 1B), bone marrow, spleen, PLNs,  
144 MLNs, and colonic mucosa (Figure 1F) from SICs versus VIRs.

145

146 Cell-associated SIV-DNA levels closely mirrored the dynamics of CD4<sup>+</sup> T-cells. Similarly high  
147 levels of cell-associated SIV-DNA were observed in RBs from SICs and VIRs during primary  
148 infection, but lower levels were observed in RBs from SICs *versus* VIRs during chronic  
149 infection (Figure 1G). Of note, SIV-DNA levels were already approximately 1 log lower in  
150 PLNs *versus* RBs from SICs during primary infection, and accordingly, lower levels were  
151 observed in PLNs from SICs *versus* VIRs since day 14 *p.i.* (Figure 1H). This finding suggests  
152 that early viral replication may be contained more efficiently in lymphoid nodes in SICs  
153 compared with other explored anatomical compartments. SIV-DNA was also detected in  
154 alveolar macrophages from all CyMs throughout the course of infection, again at lower  
155 levels in SICs *versus* VIRs during chronic infection (Figure S1B). In addition, SIV-DNA levels  
156 tended to decline progressively over time in SICs in all tissues analyzed, whereas SIV-DNA  
157 levels remained stable after primary infection in VIRs (Figure 1C, G, H). At the time of  
158 euthanasia, SIV-DNA levels were substantially lower in blood (Figure 1C), bone marrow,  
159 PLNs, MLNs, and gut mucosa (Figure 1I and Figure S1C) from SICs *versus* VIRs.

160

161 Collectively, these data indicate that progressive systemic control of viral replication is  
162 achieved in SICs with CD4<sup>+</sup> T-cell preservation and lower pan-anatomical reservoirs of SIV-  
163 DNA. Our results also underline the early preservation of PLNs in these animals.

164

165 ***The dynamics of CD8<sup>+</sup> T-cell expansion and activation do not predict control of SIV***

166 To understand the mechanisms that contribute to immune control of SIV, we first monitored  
167 the proliferation and activation dynamics of total CD8<sup>+</sup> T-cells in blood and lymphoid tissues  
168 from SICs and VIRs. Recent studies in hyperacute HIV infected individuals indicate that the  
169 changes observed in the total CD8<sup>+</sup> T-cell activation during acute infection may be largely  
170 related to changes in the HIV-specific CD8<sup>+</sup> T-cell pool (Ndhlovu et al., 2015; Takata et al.,  
171 2017). The frequencies of CD8<sup>+</sup> T-cells expressing Ki-67 in blood increased to maximum levels  
172 during primary infection (measured peak at day 15 *p.i.*), coinciding with the measured peak  
173 of viremia, then declined steadily to baseline levels during chronic infection (Figure 2A).  
174 Similar dynamics were observed in PLNs (Figure 2B) and gut mucosa (Figure 2C). In general,  
175 there were no significant differences between SICs and VIRs with respect to the dynamics of  
176 Ki-67 expression within the CD8<sup>+</sup> T-cell pool, although lower frequencies of CD8<sup>+</sup> T-cells  
177 expressing Ki-67 were observed during chronic infection in PLNs from SICs *versus* VIRs  
178 (Figure 2B).

179  
180 The frequencies of CD8<sup>+</sup> T-cells expressing the activation markers CD38 and HLA-DR in blood,  
181 PLNs, and gut mucosa increased similarly during primary infection (measured peak at day 28  
182 *p.i.*), following the dynamics of Ki-67 expression in the same compartments (Figure 2D–F).  
183 Again, there were no significant differences between SICs and VIRs with respect to the early  
184 dynamics of total CD8<sup>+</sup> T-cell activation, but lower frequencies of CD8<sup>+</sup> T-cells expressing  
185 CD38 and HLA-DR were observed during chronic infection in PLNs from SICs *versus* VIRs  
186 (Figure 2E).

187  
188 Overall, our findings indicate that although lower activation and proliferation is observed in  
189 of CD8<sup>+</sup> T-cells from SICs than VIRs in the chronic stage of infection, the early proliferation

190 and activation dynamics of the total pool of CD8<sup>+</sup> T-cells do not distinguish subsequent  
191 progression rates.

192

193 ***SIV-specific CD8<sup>+</sup> T-cell frequencies do not predict control of SIV***

194 We analyzed CD8<sup>+</sup> T-cell responses to a pool of optimal SIVmac251 peptides, which included  
195 peptides from different SIV proteins recognized by the most frequent MHC haplotypes in  
196 CyMs (M1, M2 and M3) and by the MHC haplotype M6 (Table S3). All the animals carried at  
197 least one haplotype matching some peptide, and overall there was no difference in the  
198 number of peptides tested theoretically recognized in SICs and VIRs ( $p=0.35$ ). SIV-specific  
199 CD8<sup>+</sup> T-cells producing TNF $\alpha$  (cytokine showing the lowest background in the absence of  
200 peptide or in presence of peptide during the baseline and hence used as reference) emerged  
201 in all CyMs during primary infection, coinciding with the peak of viremia, and no significant  
202 differences were observed between SICs and VIRs with respect to the frequencies of these  
203 cells in any anatomical compartment at any stage of infection (Figure 3A). Similarly, no  
204 consistent differences were observed between SICs and VIRs with respect to the frequencies  
205 of SIV-specific CD8<sup>+</sup> T-cells that produced other cytokines, including IFN $\gamma$  (Figure S2A) and IL-  
206 2 (Figure S2B), or mobilized CD107a (Figure S2C). The overall SIV-specific CD8<sup>+</sup> T-cell  
207 response, determined in each CyM as the frequency of cells displaying at least one function  
208 (TNF $\alpha$ , IFN $\gamma$ , IL-2, or CD107a), was also equivalent between SICs and VIRs across anatomical  
209 compartments throughout infection (Figure S2D). In addition, no clear differences between  
210 SICs and VIRs were observed with respect to the frequencies of SIV-specific CD8<sup>+</sup> T-cells  
211 displaying at least three functions simultaneously in blood or PLNs during acute infection,  
212 but higher frequencies of polyfunctional SIV-specific CD8<sup>+</sup> T-cells were present during  
213 chronic infection in lymphoid tissues from SICs *versus* VIRs (Figure 3B and S2E). Of note, no

214 differences in the magnitude and polyfunction of SIV-specific CD8<sup>+</sup> T-cells from SICs and VIRs  
215 were observed either when a pool of overlapping peptides spanning SIV Gag was used  
216 instead of the optimal peptide pool to stimulate the cells (Figure S3).

217

218 These data suggest that natural control of SIV is not associated with acutely generated,  
219 functionally superior SIV-specific CD8<sup>+</sup> T-cell responses, defined on the basis of cytokine  
220 production and degranulation.

221

222 ***Progressive acquisition of CD8<sup>+</sup> T-cell-mediated SIV-suppressive activity is associated with***  
223 ***control of SIV***

224 CD8<sup>+</sup> T-cells from HICs typically suppress *ex vivo* infection of autologous CD4<sup>+</sup> T-cells (Angin  
225 et al., 2016; Buckheit et al., 2012; Julg et al., 2010; Saez-Cirion et al., 2007; Saez-Cirion et al.,  
226 2009; Tansiri et al., 2015). We therefore investigated this property as a potential  
227 discriminant between SICs and VIRs. The capacity of CD8<sup>+</sup> T-cells in blood and PLNs to  
228 suppress infection of autologous CD4<sup>+</sup> T-cells was relatively weak in all CyMs during acute  
229 infection (Figure 4A), but this activity correlated negatively with VL on day 15 *p.i.* (Figure 4B,  
230 upper panel) suggesting its contribution to control viremia since early time points.  
231 Interestingly, the CD8<sup>+</sup> T-cell-mediated SIV-suppressive activity increased substantially over  
232 time in SICs (Figure 4A and S4A), either in blood or tissues. No such acquisition of SIV-  
233 suppressive activity was observed in VIRs (Figure 4A and S4A). Moreover, CD8<sup>+</sup> T-cell-  
234 mediated SIV-suppressive activity on day 70 *p.i.* correlated negatively (or tended to  
235 correlate) with subsequent determinations of plasma VL (Figure S4B) and there was a  
236 negative correlation between the CD8<sup>+</sup> T-cell-mediated SIV-suppressive activity at  
237 euthanasia and the VL at this time (Figure 4C, upper panels). In contrast, we never found

238 negative correlations between VL (at any given time) and the suppressive capacity of CD8<sup>+</sup> T-  
239 cells measured at subsequent time points. No significant correlations were identified at any  
240 time point between SIV-specific CD8<sup>+</sup> T-cell frequencies, categorized according to TNF $\alpha$   
241 production in response to SIV peptides, and measurements of plasma VL (Figure 4B-C, S4B  
242 bottom panels). Moreover, CD8<sup>+</sup> T-cell-mediated SIV-suppressive activity across the entire  
243 follow-up period, quantified as area under the curve, tended to correlate negatively with  
244 plasma VL ( $r_s = -0.47$ ,  $p = 0.07$ ), whereas no such association was identified for the  
245 frequency of SIV-specific CD8<sup>+</sup> T-cells ( $r_s = -0.01$ ,  $p = 0.97$ ) (Figure 4D). All these results  
246 indicate that changes in the suppressive capacity of CD8<sup>+</sup> T-cell, but not in the frequency of  
247 SIV-specific CD8<sup>+</sup> T-cells were associated with SIV control. We have previously shown that  
248 strong HIV-suppressive capacity of CD8<sup>+</sup> T-cells from HIV-1 controllers was linked to their  
249 ability to rapidly eliminate *ex vivo* autologous infected cells through cytotoxic mechanisms  
250 (Saez-Cirion et al., 2007). Although we could not repeat here all the analyses we did in our  
251 studies in cohorts of HIV controllers, we could confirm that the capacity of CD8<sup>+</sup> T-cells to  
252 suppress SIV infection *ex vivo* required contact with infected CD4<sup>+</sup> T-cells, and it was lost  
253 when CD8<sup>+</sup> and CD4<sup>+</sup> T-cells were separated by transwell membranes (Figure S5A).

254

255 Our results exposed a disconnection between the development of SIV-specific CD8<sup>+</sup> T-cells  
256 responding to SIV peptides and the ability of these cells to suppress SIV infection, as  
257 measured in our viral inhibition assay *ex vivo* (Figure 4E, Figure S4A). SIV-specific CD8<sup>+</sup> T-cell  
258 frequencies increased sharply as the initial viremia began to fall and remained high for the  
259 duration of the study in CyMs irrespectively of their level of viremia. However, the  
260 substantial decline in viremia to levels below 400 copies/mL in SICs coincided with the raise  
261 of SIV-suppressive activity. The increase of CD8<sup>+</sup> T-cell-mediated SIV-suppressive activity was

262 delayed in the late controller #BL669 and #BO413, but nonetheless preceded optimal control  
263 of VL in these CyMs (Figure S4A). A very strong capacity of CD8<sup>+</sup> T-cells to suppress SIV was  
264 observed at day 36 in the LN from two animals (BA209 and BC657) that did not show such  
265 capacity in the blood (Figure 4A). Only one animal (29925) did not develop any detectable  
266 SIV suppressive activity during our follow up. This animal had the weakest peak of viremia (1  
267 log lower than any other) and achieved the fastest control (Figure S4A). Whether a very  
268 rapid or local development of the CD8<sup>+</sup> T-cell suppressive capacity may have occurred or  
269 other mechanisms were associated with control of viremia in this animal remains unknown.  
270 At the time of euthanasia, superior CD8<sup>+</sup> T-cell-mediated SIV-suppressive activity was  
271 detected in a vast majority of SICs across all anatomical compartments, with the exception  
272 of bone marrow (Figure 4A), which nonetheless harbored SIV-specific CD8<sup>+</sup> T-cells at  
273 frequencies comparable to other tissues (Figure 3A). Thus, although abundant, SIV-specific  
274 CD8<sup>+</sup> T-cells induced during primary SIV infection had limited SIV suppressive capacity when  
275 compared to cells found at later time points in SICs.

276

277 One limitation of our study was the reduced number of viremic animals we could compare in  
278 parallel to SICs. To confirm that the capacity of CD8<sup>+</sup> T-cells to suppress *ex vivo* SIV infection  
279 did not increase in VIRs, we analyzed this activity in an additional group of 14 non-M6 CyMs  
280 infected intravenously (*i.v.*) with 1,000AID<sub>50</sub> of SIVmac251 and characterized by high  
281 setpoint viremia (ANRS pVISCANTI study). In these animals, the CD8<sup>+</sup> T-cell-mediated SIV-  
282 suppressive activity also remained modest throughout the follow-up (Figure S6A). The  
283 combined analysis of the CD8<sup>+</sup> T-cells from all VIRs (n=4 50AID<sub>50</sub> + n=14 1,000AID<sub>50</sub>) exposed  
284 early significant differences in the CD8<sup>+</sup> T-cell-mediated SIV-suppressive activity when  
285 compared to the SICs (p=0.052 at day 36 *p.i.* and p<0.05 at days 70 and 169 *p.i.*, Figure S6B),

286 and significantly higher capacity to suppress SIV infection of CD8<sup>+</sup> T-cells from SICs than cells  
287 from VIRs in all tissues analyzed at the end of the study (Figure S6B). Moreover, early  
288 initiation (day 28 post-infection) of antiretroviral treatment in another group of CyM  
289 inoculated with 1,000AID<sub>50</sub> of SIVmac251 sharply decreased VL and CD8<sup>+</sup> T-cell activation  
290 levels (Figure S6C) but did not change the capacity of CD8<sup>+</sup> T-cells from these animals to  
291 suppress infection *ex vivo*, which remained extremely weak (Figure S6C). These results,  
292 which are in agreement with our previous observations in early treated HIV-infected  
293 individuals (Lecuroux et al., 2013), show that low SIV suppressive capacity during acute  
294 infection was neither a consequence of strong activation of these cells *in vivo* nor of high  
295 antigen burden.

296

297 Finally, one possible explanation for the weak SIV suppressive capacity of CD8<sup>+</sup> T-cells from  
298 VIRs was that they had a limited capacity to recognize the SIVmac251 we used in our viral  
299 inhibition assay, due to potential adaptation of the CD8<sup>+</sup> T-cell response to evolving viruses  
300 in these CyMs. However, CD8<sup>+</sup> T-cells from VIRs were not able to eliminate either the CD4<sup>+</sup> T-  
301 cells that produced “autologous” SIV upon activation *in vitro*. In contrast, although CD8<sup>+</sup> T-  
302 cells from SICs were not able to suppress autologous virus during early infection, they  
303 acquired this capacity progressively at the same rate we found in our classical protocol  
304 (Figure S5B). These results confirmed that CD8<sup>+</sup> T-cells from SICs and VIRs had functional  
305 differences that were unlinked to the evolution of the infecting virus.

306

307 Collectively, our results show that the capacity of SIV-specific CD8<sup>+</sup> T-cells to suppress  
308 infection *ex vivo* was a genuine quality that progressively amplified in SICs. Our results

309 further uncover a temporal link between the acquisition by CD8<sup>+</sup> T-cells of potent capacity to  
310 suppress infection and sustained control of SIV.

311

312 ***Acquisition of CD8<sup>+</sup> T-cell-mediated SIV-suppressive activity in SICs occurs independently of***  
313 ***MHC haplotype***

314 Our primary intention in this study was to explore the mechanisms underlying natural  
315 control of SIV infection, independently of MHC background or infectious dose. However, as  
316 expected (Bruel et al., 2015), inoculation with low-dose virus and carriage of the protective  
317 M6 haplotype independently favored spontaneous control of viremia below 400 copies/mL  
318 in CyMs in our study (Table S4, Figure S7A). We therefore evaluated whether these  
319 parameters influenced the dynamics of control and the development of the CD8<sup>+</sup> T-cell  
320 response upon infection. We found that CD4<sup>+</sup> T-cells and the levels of cell-associated SIV-  
321 DNA similarly evolved in the blood and PLNs from M6 and non-M6 controllers (Figure S7B).  
322 There was just a tendency for M6 controllers *versus* non-M6 controllers to a better recovery  
323 of CD4<sup>+</sup> T-cells in blood at the end of the study (p=0.07). Similarly, we did not find important  
324 differences between M6 and non-M6 controllers in their development of SIV-specific CD8<sup>+</sup> T-  
325 cell responses (Figure S7C). M6 and non-M6 controllers developed similar frequencies of SIV-  
326 responding cells during acute infection that were maintained during the follow up. Of note,  
327 the capacity of CD8<sup>+</sup> T-cells to suppress *ex vivo* SIV infection of CD4<sup>+</sup> T-cells progressively  
328 increased in both M6 and non-M6 SICs. The only difference that we could appreciate was a  
329 faster acquisition (day 36 *p.i.*) of CD8<sup>+</sup> T-cell mediated SIV suppressive activity in the PLN  
330 from M6 SICs *versus* non-M6 SICs (Figure S7C). Intriguingly, non-M6 SICs had higher  
331 frequencies of SIV responding CD8<sup>+</sup> T-cells in this tissue at the same time point. Overall these  
332 results show that while the M6 background gave a selective advantage to CyMs to control

333 infection in conditions of higher viral inoculum, this MHC haplotype was not indispensable  
334 for the acquisition of SIV suppressive capacity by CD8<sup>+</sup> T-cells, which occurred both in M6  
335 and non-M6 SICs. The results are in agreement with the observations in HIV controllers.  
336 Although cohorts of HICs are enriched in individuals carrying protective HLA class I alleles  
337 (mainly HLA-B\*57, B\*27), many HICs do not carry protective HLA class I alleles but have CD8<sup>+</sup>  
338 T-cells with strong HIV suppressive capacity *ex vivo* (Lecuroux et al., 2014). Therefore, the  
339 development of efficient CD8<sup>+</sup> T-cell responses with antiviral activity is a characteristic of  
340 most HICs/SICs, independently of their MHC background.

341

342 ***Skewed maturation of central memory SIV-specific CD8<sup>+</sup> T-cells is associated with defective***  
343 ***acquisition of SIV-suppressive activity***

344 To dissect the phenotypic correlates of *ex vivo* measured antiviral potency, we analyzed the  
345 differentiation status of SIV-specific CD8<sup>+</sup> T-cells using selected markers in conjunction with  
346 MHC class I tetramers. Tetramer-binding SIV-specific CD8<sup>+</sup> T-cells were detected in all CyMs,  
347 displayed early similar differentiation profiles in SICs and VIRs, but evolved differently, such  
348 that higher frequencies of central memory (CM) SIV-specific CD8<sup>+</sup> T-cells were present in  
349 SICs versus VIRs on day 105 *p.i.* ( $p = 0.018$ ) and day 535 *p.i.* ( $p = 0.013$ ) (Figure 5A, B).

350

351 In further analyses, we found that higher frequencies of SIV-specific CD8<sup>+</sup> T-cells from SICs  
352 expressed the IL-7 receptor CD127, which is associated with cell survival and memory  
353 responses (Schluns et al., 2000), whereas higher frequencies of SIV-specific CD8<sup>+</sup> T-cells from  
354 VIRs expressed the transcription factor T-bet, which is associated with cellular differentiation  
355 and effector functionality (Sullivan et al., 2003; Szabo et al., 2002) (Figure 6A). These  
356 differences seemed to appear since primary infection, but due to the limited number of VIRs

357 analyzed, the differences only reached statistical significance at later time points (Figure 6A).  
358 Expression levels of CD127 and T-bet also varied as a function of differentiation among SIV-  
359 specific CD8<sup>+</sup> T-cells from SICs and VIRs (Figure 6B). In particular, CM and transitional  
360 memory (TM) SIV-specific CD8<sup>+</sup> T-cells expressed lower levels of T-bet throughout the course  
361 of infection in SICs *versus* VIRs, whereas CM SIV-specific CD8<sup>+</sup> T-cells tended to express  
362 higher levels of CD127 during chronic infection in SICs *versus* VIRs.

363

364 To palliate the limited statistical power, we analyzed all animals together, taking into  
365 account the spectrum of outcomes rather than group classifications. We found negative  
366 correlations during primary infection and at euthanasia between the expression levels of  
367 CD127 on SIV-specific CD8<sup>+</sup> T-cells and plasma VLs (Figure 7A). Of note, the levels of CD127  
368 correlated positively with CD8<sup>+</sup> T-cell-mediated SIV-suppressive activity at the same time  
369 points (Figure 7B). On the contrary, negative correlations were observed during primary  
370 infection and at euthanasia between CD8<sup>+</sup> T-cell-mediated SIV-suppressive activity and the  
371 contemporaneous frequencies of T-bet<sup>+</sup>CD127<sup>-</sup>SIV-specific CD8<sup>+</sup> T-cells (Figure 7C) and  
372 between CD8<sup>+</sup> T-cell-mediated SIV-suppressive activity and expression levels of T-bet among  
373 CM SIV-specific CD8<sup>+</sup> T-cells (Figure 7D).

374

375 Altogether, these results point to the importance of the early establishment and  
376 maintenance of optimal memory CD8<sup>+</sup> T-cell responses for achieving viral control. Recently,  
377 the presence of a population of memory-like CD8<sup>+</sup> T-cells with stem cell-like properties,  
378 characterized by the expression of the transcription factor 1 (TCF-1) (Zhou et al., 2010), was  
379 shown to be critical to sustain the CD8<sup>+</sup> T-cell response against chronic viral infections (Snell  
380 et al., 2018; Utzschneider et al., 2016). We found that SIV-specific CM CD8<sup>+</sup> T-cells from SICs

381 expressed higher levels of TCF-1 than cells from VIRs (Figure 7E). Among TCF-1 expressing  
382 cells, a higher frequency of cells from SICs expressed in addition CXCR5 and CCR7, revealing  
383 the presence of memory-like responses with the potential capacity to migrate to the lymph  
384 node follicles (Leong et al., 2016).

385

386 Collectively, these results suggest that SICs developed during early infection SIV-specific  
387 CD8<sup>+</sup> T-cells that enabled long-term memory potential, sustained antiviral activity and viral  
388 control, whereas the corresponding SIV-specific CD8<sup>+</sup> T-cells in VIRs adopt a skewed  
389 phenotype associated with cellular differentiation, suboptimal antiviral activity and more  
390 prone to exhaustion (Zhou et al., 2010).

391 **DISCUSSION**

392 This study provides insights into the immune correlates of natural SIV control. Although SIV-  
393 specific CD8<sup>+</sup> T-cells were generated during acute infection with equivalent dynamics and  
394 global frequencies in all CyMs, preventing discrimination between SICs and VIRs, antiviral  
395 efficacy *ex vivo* developed progressively over time and was associated with spontaneous SIV  
396 control. This dichotomy was underpinned by distinct early memory programs within the SIV-  
397 specific CD8<sup>+</sup> T-cell pool. Collectively, these findings identify a cohesive set of immunological  
398 parameters that associate with effective and sustained control of SIV.

399

400 To monitor the establishment of natural control prospectively, we took advantage of  
401 previous reports showing that carriage of the MHC haplotype M6 and *i.r.* inoculation with  
402 low-dose (5AID<sub>50</sub>) virus independently favor spontaneous control of SIVmac251 infection in  
403 CyMs (Aarnink et al., 2011; Bruel et al., 2015; Mee et al., 2009). Our results corroborate  
404 previous reports. In particular, although the presence M6 haplotype favored more frequent  
405 and more rapid control of infection among animals receiving a high dose of the virus  
406 (50AID<sub>50</sub>) (Table S4), no significant differences were observed in the dynamics of SIV control  
407 in M6 and non-M6 SICs. At the time of euthanasia, a higher proportion of CD4<sup>+</sup> T-cells and  
408 lower cell-associated SIV-DNA levels were found in multiple tissues from SICs *versus* VIRs,  
409 demonstrating systemic control of SIV. These differences were much more subtle during  
410 primary infection. However, PLNs from SICs harbored approximately 10-fold less SIV-DNA in  
411 the acute phase than PLNs from VIRs. In addition, the frequency of CD4<sup>+</sup> T-cells were  
412 maintained close to baseline throughout the course of the study in PLNs, but not in blood or  
413 RBs, from SICs. These observations suggest that early containment of viral replication in LNs

414 (Buggert et al., 2018; Reuter et al., 2017) may be a key event for subsequent immune control  
415 of SIV.

416

417 In line with previous studies in humans (Lecuroux et al., 2013; Ndhlovu et al., 2015;  
418 Trautmann et al., 2012) and non-human primates (Veazey et al., 2001) we observed early  
419 and robust expansions of SIV-specific CD8<sup>+</sup> T-cells in all CyMs. However, the functional  
420 profiles and overall frequencies of SIV-specific CD8<sup>+</sup> T-cells (as determined by intra cellular  
421 cytokine staining upon SIV antigen stimulation) during the acute phase of infection were  
422 largely equivalent in SICs and VIRs, and neither parameter correlated with subsequent  
423 determinations of plasma VL. Similarly, the functional profiles and overall frequencies of SIV-  
424 specific CD8<sup>+</sup> T-cells during the chronic phase of infection were largely equivalent in SICs and  
425 VIRs, although polyfunctionality (defined as the capacity to produce simultaneously several  
426 cytokine and/or degranulate) was impaired at the time of euthanasia in VIRs. These results  
427 suggest that differences in polyfunctionality found during chronic infection are a surrogate  
428 marker of viral replication rather than an accurate determinant of antiviral efficacy, although  
429 low number of animals in the VIR group may limit statistical power.

430

431 The capacity of CD8<sup>+</sup> T-cells to suppress infection of autologous CD4<sup>+</sup> T-cells directly *ex vivo*  
432 is a particular feature of HICs (Almeida et al., 2009; Angin et al., 2016; Buckheit et al., 2012;  
433 Julg et al., 2010; Saez-Cirion et al., 2007; Saez-Cirion et al., 2009; Tansiri et al., 2015) that is  
434 mediated by the rapid elimination of infected CD4<sup>+</sup> T-cells through MHC-restricted  
435 mechanisms (Saez-Cirion et al., 2007). Irrespective of subsequent outcome, we detected  
436 relatively weak CD8<sup>+</sup> T-cell-mediated SIV-suppressive activity during primary infection,  
437 despite the vigorous mobilization of SIV-specific CD8<sup>+</sup> T-cells. This observation parallels our

438 previous findings in the setting of HIV (Lecuroux et al., 2013) and point to limited antiviral  
439 potential of CD8<sup>+</sup> T-cell responses generated during primary infection. However, a negative  
440 correlation was already observed between the CD8<sup>+</sup> T-cell-mediated SIV-suppressive activity  
441 and viremia at this early time point, showing early temporal association of this antiviral  
442 activity and reduction of viremia. Of note, this SIV-suppressive capacity of CD8<sup>+</sup> T-cells  
443 increased progressively over a period of weeks in some animals, carrying or not the  
444 protective MHC haplotype M6. At the time of euthanasia, these highly potent antiviral CD8<sup>+</sup>  
445 T-cells were present in all tissues in SICs, with the exception of bone marrow, where this  
446 activity tended to be higher in SICs but overall weaker than in other tissues. It is important to  
447 notice that CD8<sup>+</sup> T-cell-mediated SIV suppression was very weak also in PLNs during the first  
448 weeks following infection but increased over time in SICs. Therefore, the increase in the  
449 capacity of CD8<sup>+</sup> T-cells to suppress infection was not the result of the recirculation of CD8<sup>+</sup>  
450 T-cells from LNs once control was established, but a genuine progressive augmentation of  
451 the antiviral potential of the cells. The development of potent antiviral CD8<sup>+</sup> T-cells is  
452 therefore a *bone fide* correlate of sustained control of SIV.

453

454 We provide several arguments supporting that the progressive enhancement of the capacity  
455 of CD8<sup>+</sup> T-cells to suppress SIV infection led to the establishment of controlled viremia,  
456 rather than evolving as a consequence of viral control. As the dynamics of control were not  
457 homogeneous, we established a mathematical model to predict the development of  
458 effective immune-mediated control of SIV in our study (Madelain et al., 2020). Importantly,  
459 the model was constructed using exclusively SIV-RNA and SIV-DNA data from VIRs and SICs.  
460 SIV-RNA kinetics were best fitted using a model where the cytotoxic immune response  
461 progressively mounted up. The model predicted that faster decay in VL in SICs was

462 associated with a progressive development of a cytotoxic CD8<sup>+</sup> T-cell response that  
463 decreased over ten times the half-life of infected cells (from 5.5 days to 0.3 days). The model  
464 also predicted that in SICs the maximal level of cytotoxic response was reached within 100  
465 days of infection. Interestingly, the predictions of the kinetics of development of cytotoxic  
466 CD8<sup>+</sup> T-cell responses matched, in *post-hoc* analyses, with the values of the capacity of CD8<sup>+</sup>  
467 T-cells to suppress infection that we obtained experimentally, but not with the frequency of  
468 CD8<sup>+</sup> T-cells that responded to SIV peptides. Moreover, we found that SIV suppressive  
469 activity of CD8<sup>+</sup> T-cells 70 days after infection correlated negatively with ulterior VLs, while  
470 the suppressive activity never correlated negatively with preceding VLs. Control of viremia  
471 driven by antiretroviral treatment, did not lead to the development of SIV suppressive  
472 activity by CD8<sup>+</sup> T-cells. Therefore, the enhancement of SIV suppressive capacity does not  
473 occur in response to a decrease in antigen levels.

474

475 Due to limited longitudinal sampling in lymphoid tissues, we cannot exclude, however, that  
476 SIV control or emergence of SIV suppressive capacity by CD8<sup>+</sup> T-cells in these tissues,  
477 preceded our observations. Moreover, the progressive establishment of control of infection  
478 and maturation of the CD8<sup>+</sup> T-cell response might be the result of a virtuous circle, in which  
479 initial reduced dynamics of viral replication in LNs allowed the development of more  
480 effective CD8<sup>+</sup> T-cell responses, which in turn drove a steeper reduction in viremia.  
481 “Goldilocks” levels of viral replication might then allow CD8<sup>+</sup> T-cells to attain their maximal  
482 antiviral potential and sustain viral control, as has been proposed to occur in CMV infection  
483 (Picker, 2014).

484

485 Interestingly, CD8<sup>+</sup> T-cells that can control certain “latent” chronic viral infections, such as  
486 CMV or EBV, do not show features of functional exhaustion when compared to CD8<sup>+</sup> T-cells  
487 against other chronic viral infections such as SIV/HIV, HCV or HBV (Chatterjee et al., 2019;  
488 Fenwick et al., 2019; Luxenburger et al., 2018; van den Berg et al., 2019; Ye et al., 2015). This  
489 appears to be related to the development of CD8<sup>+</sup> T-cells with distinct molecular programs  
490 that allow long-term memory and the replenishment of the effector compartment in  
491 reponse to antigenic stimulation (Paley et al., 2012). Recent studies have identified a subset  
492 of memory-like CD8<sup>+</sup> T-cells that express the transcription factor TCF-1 as responsible for  
493 sustaining the immune response against chronic viral infections (Utzschneider et al., 2016).  
494 CD8<sup>+</sup> T-cells expressing TCF-1 have characteristics of central memory cells, possess strong  
495 proliferative potential and are able to produce more differentiated cell subset, while being  
496 less prone to exhaustion after repeated antigenic stimulation (Snell et al., 2018;  
497 Utzschneider et al., 2016; Zhou et al., 2010). We found that SIV-specific CD8<sup>+</sup> T-cells from  
498 SICs expressed higher levels of TCF-1 than cells from VIRs, and these differences were more  
499 visible among less differentiated subsets, and coupled with an enhanced expression of  
500 CXCR5, which may reflect the potential of these cells to migrate to germinal centers. During  
501 the revision of this manuscript, a preprint became available describing similar findings in  
502 cells from both HIV and SIV controllers in an independent study (Rutishauser et al., 2020). In  
503 that study, the authors linked the expression of TCF-1 with the capacity of HIV-specific CD8<sup>+</sup>  
504 T-cells to expand.

505

506 One decisive characteristic for the establishment of long-term memory is the capacity to  
507 upregulate the IL-7 receptor  $\alpha$ -subunit (CD127) (Huster et al., 2004). In addition, studies in  
508 mice have shown that decreased expression of T-bet among memory CD8<sup>+</sup> T-cells allows the

509 establishment of long-lived CD127<sup>hi</sup> cells, which maintain the capacity to proliferate and  
510 control successive infections (Joshi et al., 2007; Joshi et al., 2011). In our study, the  
511 divergent outcome of SICs *versus* VIRs was preceded by early differences in the expression of  
512 CD127 and T-bet, especially within the less differentiated memory pool (CM and TM). In  
513 particular, at day 21 post-infection, higher frequencies of SIV-specific CM CD8<sup>+</sup> T-cells  
514 expressed CD127 in SICs, whereas higher frequencies of SIV-specific CM and TM CD8<sup>+</sup> T-cells  
515 expressed T-bet in VIRs. It is important to note that plasma viremia was uncontrolled at this  
516 time point and largely equivalent in animals that became SICs (median 5.19 log SIV RNA) or  
517 VIRs (median 5.36, p=0.65). The phenotypic differences remained consistent, or even  
518 appeared to become more pronounced throughout the course of infection, although the  
519 statistical power of the analyses was affected by the limited number of VIRs studied. Overall,  
520 our data suggest that SICs develop very early memory-like SIV-specific CD8<sup>+</sup> T-cell responses,  
521 whereas VIRs develop SIV-specific memory CD8<sup>+</sup> T-cell responses skewed towards more  
522 effector-like characteristics and that these differences may be determinant to achieving and  
523 sustaining viral control. These findings are broadly consistent with several previous reports  
524 describing immune profiles that associate with the control of viremia in HICs during chronic  
525 infection. Favorable characteristics include high frequencies of CD57<sup>+</sup> eomesodermin<sup>hi</sup> HIV-  
526 specific CD8<sup>+</sup> T-cells with superior proliferative capacity, increased expression levels of  
527 CD127, and intermediate expression levels of T-bet (Simonetta et al., 2014), and high  
528 frequencies of HIV-specific CD8<sup>+</sup> T-cells with the capacity to upregulate T-bet, granzyme B,  
529 and perforin in response to antigen encounter (Hersperger et al., 2011b; Migueles et al.,  
530 2008).

531

532 In a recent single cell study (Angin et al., 2019), we also found differences in the program of  
533 HIV-specific CM CD8<sup>+</sup> T-cells from HICs and non-controllers: whereas HIV-specific CM CD8<sup>+</sup> T-  
534 cells from HICs upregulated the expression of effectors genes linked with mTORC2 activation  
535 and cell survival (including CD127), CM cells from non-controllers had a skewed profile  
536 associated with mTORC1 activation (including T-bet) and glycolysis. This was traduced in a  
537 dependency on glucose of HIV-specific CD8<sup>+</sup> T-cells from non-controllers to react to HIV  
538 antigens, while HIV-specific CD8<sup>+</sup> T-cells from HICs were characterized by metabolic plasticity  
539 and being able to exert their function even in conditions of glucose deprivation. Of note,  
540 these differences in the metabolic program of cells from controllers and non-controllers  
541 could also be recapitulated with SIV-specific CD8<sup>+</sup> T-cells from SICs and VIR macaques from  
542 the present study (Angin et al., 2019), further corroborating the validity of our CyM model to  
543 study the development of the protective CD8<sup>+</sup> T-cell responses characteristics of HIV/SIV  
544 controllers. The present results extend these observations and support a key role for long-  
545 lived memory responses in the control of SIV. Importantly, our data also show that distinct  
546 memory responses are formed early after infection, potentially reflecting different priming  
547 conditions.

548

549 Several important questions remain unresolved. It remains unclear which factors are  
550 required to encourage the development of memory CD8<sup>+</sup> T-cell responses that provide  
551 optimal protection against HIV/SIV. In some viral infections, expression of T-bet is tightly  
552 regulated by cytokines, such as IL-12 (Rao et al., 2012; Takemoto et al., 2006). A recent study  
553 in the LCMV murine model of infection suggests that memory-like TCF-1 CD8<sup>+</sup> T-cell  
554 responses with stemness potential and enhanced capacity to react upon secondary  
555 challenge, are developed during early chronic infection (in an immunosuppressive

556 environment), while memory cells that are developed at the onset of infection (in a pro-  
557 inflammatory environment) become short-term effectors and are rapidly exhausted (Snell et  
558 al., 2018). Based on these observations we propose that balanced inflammatory responses  
559 (Barouch et al., 2016) arising as a consequence of lower viral burdens in lymph nodes during  
560 acute infection in SICs might facilitate antigen-specific priming events associated with  
561 optimal memory programs (Ozga et al., 2016) and minimize the loss of CD4<sup>+</sup> T-cells, which  
562 provide helper functions that are critical for the development of long-lived memory-like  
563 CD8<sup>+</sup> T-cells (Khanolkar et al., 2004; Utzschneider et al., 2016). It is unclear, however, which  
564 mechanisms were responsible for the reduced viral dynamics in the lymph nodes of SICs  
565 during acute infection. In the case of animals carrying the M6 haplotype, this could be  
566 related to more effective NK cell responses, as has been shown for humans carrying some  
567 protective HLA alleles (Martin et al., 2002). For animals inoculated with a lower dose of the  
568 virus this could be due to a lower diversity of infecting viruses (Liu et al., 2010), which could  
569 limit the inflammatory response and be more efficiently controlled by initial CD8<sup>+</sup> T-cell  
570 responses. Although we have shown that the changes in the suppressive capacity of CD8<sup>+</sup> T-  
571 cells were related to intrinsic functional properties of the cells and not to different capacities  
572 to react against evolving viruses, a better understanding of the evolution of viral diversity  
573 and the quality of immune responses appears important in sight of our results. Finally, we  
574 found that the proportion of CD127<sup>+</sup> SIV-specific CD8<sup>+</sup> T-cells during acute and chronic  
575 infection correlated positively with CD8<sup>+</sup> T-cell-mediated SIV-suppressive activity and we  
576 propose that the amplification of potent antiviral activity is the result of a maturation  
577 process, the trajectory of which is linked to the early optimal programming of the CD8<sup>+</sup> T-cell  
578 memory compartment. However, we do not have any direct evidence at the molecular level  
579 to explain why/how the capacity to suppress infection increased progressively among CD8<sup>+</sup>

580 T-cells. It is interesting to note that maturation through persistent or repeated exposure to  
581 antigen can drive the selection of specific clonotypes bearing high-affinity T-cell receptors  
582 (TCRs) (Busch and Pamer, 1999; Ozga et al., 2016; Price et al., 2005) which have been shown  
583 to suppress HIV replication more efficiently than clonotypes targeting the same antigen via  
584 low-affinity TCRs (Almeida et al., 2007; Almeida et al., 2009; Ladell et al., 2013; Lima et al.,  
585 2020). Increase in antigen sensitivity over time would be compatible with the progressive  
586 increase in antiviral potency that we observed for the CD8<sup>+</sup> T-cells from controllers in our  
587 study.

588

589 Collectively, the data presented here underscore the importance of early host-pathogen  
590 interactions in the development of adaptive immunity and reveal an optimal maturation  
591 pathway associated with the generation and maintenance of potent and sustained antiviral  
592 CD8<sup>+</sup> T-cell responses, which in turn dictate the outcome of infection with SIV.

593 **ACKNOWLEDGMENTS**

594 This study was funded by the French National Agency for research on AIDS and Viral  
595 Hepatitis (ANRS) and by MSDAvenir. Additional support was provided by the Programme  
596 Investissements d’Avenir (PIA), managed by the ANR under reference ANR-11-INBS-0008,  
597 funding the Infectious Disease Models and Innovative Therapies (IDMIT, Fontenay-aux-  
598 Roses, France) infrastructure, and ANR-10-EQPX-02-01, funding the FlowCyTech Facility  
599 (IDMIT, Fontenay-aux-Roses, France). C.P. was supported by an ANRS Postdoctoral  
600 Fellowship, A.M. was supported by MSDAvenir, and D.A.P. was supported by a Wellcome  
601 Trust Senior Investigator Award. We thank Benoit Delache, Brice Targat, Claire Torres,  
602 Christelle Cassan, Jean-Marie Robert, Julie Morin, Patricia Brochard, Sabrina Guenounou,  
603 Sebastien Langlois, and Virgile Monnet for expert technical assistance, Antonio Cosma for  
604 helpful discussion, Lev Stimmer for anatomopathology expertise, Isabelle Mangeot-Méderlé  
605 for helpful project management at IDMIT, and Christophe Joubert for veterinarian assistance  
606 at the animal facility at CEA. The SIV1C cell line was kindly provided by François Villinger. The  
607 SIVmac239 Gag Peptide Set was obtained through the NIH AIDS Reagent Program (Division  
608 of AIDS, NIAID, NIH). FTC, DTG, and TDF were obtained from Gilead and ViiV Healthcare  
609 through the “IAS Towards an HIV Cure” common Material Transfer Agreement.

610

611 **AUTHOR CONTRIBUTIONS**

612 C.P. and A.M. designed and performed experiments, analyzed data, and interpreted results.  
613 V.Ma., J.G., and V.A.F. analyzed data and interpreted results. V.Mo., A.D., P.V., and N.S.  
614 performed experiments and analyzed data. E.G., S.L.L., and D.A.P. produced bespoke  
615 reagents. N.D.B. and D.D. designed experiments, analyzed data, and interpreted results.  
616 D.A.P., A.B., G.P., R.L.G., O.L., M.M.T., and C.R. interpreted results. B.V. and A.S.C. designed

617 experiments, analyzed data, interpreted results, and supervised the study. C.P., B.V., and  
618 A.S.C. wrote the paper with assistance from A.M., V.Ma., V.Mo., A.D., P.V., N.S., D.A.P.,  
619 N.D.B., R.L.G., O.L., M.M.T., C.R., J.G., and V.A.F.

620

621 **DECLARATION OF INTERESTS**

622 The authors declare no competing interests.

- 624 Aarnink, A., Dereuddre-Bosquet, N., Vaslin, B., Le Grand, R., Winterton, P., Apoil, P.A., and  
625 Blancher, A. (2011). Influence of the MHC genotype on the progression of experimental SIV  
626 infection in the Mauritian cynomolgus macaque. *Immunogenetics* *63*, 267-274.
- 627 Allen, T.M., O'Connor, D.H., Jing, P., Dzuris, J.L., Mothe, B.R., Vogel, T.U., Dunphy, E.,  
628 Liebl, M.E., Emerson, C., Wilson, N., *et al.* (2000). Tat-specific cytotoxic T lymphocytes  
629 select for SIV escape variants during resolution of primary viraemia. *Nature* *407*, 386-390.
- 630 Almeida, J.R., Price, D.A., Papagno, L., Arkoub, Z.A., Sauce, D., Bornstein, E., Asher, T.E.,  
631 Samri, A., Schnuriger, A., Theodorou, I., *et al.* (2007). Superior control of HIV-1 replication by  
632 CD8+ T cells is reflected by their avidity, polyfunctionality, and clonal turnover. *J Exp Med*  
633 *204*, 2473-2485.
- 634 Almeida, J.R., Sauce, D., Price, D.A., Papagno, L., Shin, S.Y., Moris, A., Larsen, M.,  
635 Pancino, G., Douek, D.C., Autran, B., *et al.* (2009). Antigen sensitivity is a major determinant  
636 of CD8+ T-cell polyfunctionality and HIV-suppressive activity. *Blood* *113*, 6351-6360.
- 637 Angin, M., Volant, S., Passaes, C., Lecuroux, C., Monceaux, V., Dillies, M.-A., Valle-Casuso,  
638 J.C., Pancino, G., Vaslin, B., Grand, R.L., *et al.* (2019). Metabolic plasticity of HIV-specific  
639 CD8+ T cells is associated with enhanced antiviral potential and natural control of HIV-1  
640 infection. *Nature Metabolism* *1*, 704-716.
- 641 Angin, M., Wong, G., Papagno, L., Versmisse, P., David, A., Bayard, C., Charmeteau-De  
642 Muylder, B., Besseghir, A., Thiebaut, R., Boufassa, F., *et al.* (2016). Preservation of  
643 Lymphopoietic Potential and Virus Suppressive Capacity by CD8+ T Cells in HIV-2-Infected  
644 Controllers. *J Immunol* *197*, 2787-2795.
- 645 Antony, J.M., and MacDonald, K.S. (2015). A critical analysis of the cynomolgus macaque,  
646 *Macaca fascicularis*, as a model to test HIV-1/SIV vaccine efficacy. *Vaccine* *33*, 3073-3083.
- 647 Barouch, D.H., Ghneim, K., Bosche, W.J., Li, Y., Berkemeier, B., Hull, M., Bhattacharyya, S.,  
648 Cameron, M., Liu, J., Smith, K., *et al.* (2016). Rapid Inflammasome Activation following  
649 Mucosal SIV Infection of Rhesus Monkeys. *Cell* *165*, 656-667.
- 650 Betts, M.R., Nason, M.C., West, S.M., De Rosa, S.C., Migueles, S.A., Abraham, J.,  
651 Lederman, M.M., Benito, J.M., Goepfert, P.A., Connors, M., *et al.* (2006). HIV  
652 nonprogressors preferentially maintain highly functional HIV-specific CD8+ T cells. *Blood*  
653 *107*, 4781-4789.
- 654 Borrow, P., Lewicki, H., Hahn, B.H., Shaw, G.M., and Oldstone, M.B. (1994). Virus-specific  
655 CD8+ cytotoxic T-lymphocyte activity associated with control of viremia in primary human  
656 immunodeficiency virus type 1 infection. *J Virol* *68*, 6103-6110.
- 657 Borrow, P., Lewicki, H., Wei, X., Horwitz, M.S., Pfeffer, N., Meyers, H., Nelson, J.A., Gairin,  
658 J.E., Hahn, B.H., Oldstone, M.B., *et al.* (1997). Antiviral pressure exerted by HIV-1-specific  
659 cytotoxic T lymphocytes (CTLs) during primary infection demonstrated by rapid selection of  
660 CTL escape virus. *Nat Med* *3*, 205-211.
- 661 Bruel, T., Hamimi, C., Dereuddre-Bosquet, N., Cosma, A., Shin, S.Y., Corneau, A.,  
662 Versmisse, P., Karlsson, I., Malleret, B., Targat, B., *et al.* (2015). Long-term control of simian  
663 immunodeficiency virus (SIV) in cynomolgus macaques not associated with efficient SIV-  
664 specific CD8+ T-cell responses. *J Virol* *89*, 3542-3556.
- 665 Buckheit, R.W., 3rd, Salgado, M., Silciano, R.F., and Blankson, J.N. (2012). Inhibitory  
666 potential of subpopulations of CD8+ T cells in HIV-1-infected elite suppressors. *J Virol* *86*,  
667 13679-13688.
- 668 Buggert, M., Nguyen, S., Salgado-Montes de Oca, G., Bengsch, B., Darko, S., Ransier, A.,  
669 Roberts, E.R., Del Alcazar, D., Brody, I.B., Vella, L.A., *et al.* (2018). Identification and  
670 characterization of HIV-specific resident memory CD8(+) T cells in human lymphoid tissue.  
671 *Sci Immunol* *3*.
- 672 Busch, D.H., and Pamer, E.G. (1999). T cell affinity maturation by selective expansion during  
673 infection. *J Exp Med* *189*, 701-710.
- 674 Carrington, M., Nelson, G.W., Martin, M.P., Kissner, T., Vlahov, D., Goedert, J.J., Kaslow, R.,  
675 Buchbinder, S., Hoots, K., and O'Brien, S.J. (1999). HLA and HIV-1: heterozygote advantage  
676 and B\*35-Cw\*04 disadvantage. *Science* *283*, 1748-1752.

677 Chatterjee, B., Deng, Y., Holler, A., Nunez, N., Azzi, T., Vanoaica, L.D., Muller, A.,  
678 Zdimerova, H., Antsiferova, O., Zbinden, A., *et al.* (2019). CD8+ T cells retain protective  
679 functions despite sustained inhibitory receptor expression during Epstein-Barr virus infection  
680 in vivo. *PLoS Pathog* 15, e1007748.

681 Chowdhury, A., Hayes, T.L., Bosinger, S.E., Lawson, B.O., Vanderford, T., Schmitz, J.E.,  
682 Paiardini, M., Betts, M., Chahroudi, A., Estes, J.D., *et al.* (2015). Differential Impact of In Vivo  
683 CD8+ T Lymphocyte Depletion in Controller versus Progressor Simian Immunodeficiency  
684 Virus-Infected Macaques. *J Virol* 89, 8677-8686.

685 Day, C.L., Kaufmann, D.E., Kiepiela, P., Brown, J.A., Moodley, E.S., Reddy, S., Mackey,  
686 E.W., Miller, J.D., Leslie, A.J., DePierres, C., *et al.* (2006). PD-1 expression on HIV-specific T  
687 cells is associated with T-cell exhaustion and disease progression. *Nature* 443, 350-354.

688 Du, V.Y., Bansal, A., Carlson, J., Salazar-Gonzalez, J.F., Salazar, M.G., Ladell, K., Gras, S.,  
689 Josephs, T.M., Heath, S.L., Price, D.A., *et al.* (2016). HIV-1-Specific CD8 T Cells Exhibit  
690 Limited Cross-Reactivity during Acute Infection. *J Immunol* 196, 3276-3286.

691 Feichtinger, H., Putkonen, P., Parravicini, C., Li, S.L., Kaaya, E.E., Bottiger, D., Biberfeld, G.,  
692 and Biberfeld, P. (1990). Malignant lymphomas in cynomolgus monkeys infected with simian  
693 immunodeficiency virus. *Am J Pathol* 137, 1311-1315.

694 Fenwick, C., Joo, V., Jacquier, P., Noto, A., Banga, R., Perreau, M., and Pantaleo, G. (2019).  
695 T-cell exhaustion in HIV infection. *Immunol Rev* 292, 149-163.

696 Hersperger, A.R., Martin, J.N., Shin, L.Y., Sheth, P.M., Kovacs, C.M., Cosma, G.L.,  
697 Makedonas, G., Pereyra, F., Walker, B.D., Kaul, R., *et al.* (2011a). Increased HIV-specific  
698 CD8+ T-cell cytotoxic potential in HIV elite controllers is associated with T-bet expression.  
699 *Blood* 117, 3799-3808.

700 Hersperger, A.R., Migueles, S.A., Betts, M.R., and Connors, M. (2011b). Qualitative features  
701 of the HIV-specific CD8+ T-cell response associated with immunologic control. *Curr Opin HIV*  
702 *AIDS* 6, 169-173.

703 Hersperger, A.R., Pereyra, F., Nason, M., Demers, K., Sheth, P., Shin, L.Y., Kovacs, C.M.,  
704 Rodriguez, B., Sieg, S.F., Teixeira-Johnson, L., *et al.* (2010). Perforin expression directly ex  
705 vivo by HIV-specific CD8 T-cells is a correlate of HIV elite control. *PLoS Pathog* 6,  
706 e1000917.

707 Huster, K.M., Busch, V., Schiemann, M., Linkemann, K., Kerksiek, K.M., Wagner, H., and  
708 Busch, D.H. (2004). Selective expression of IL-7 receptor on memory T cells identifies early  
709 CD40L-dependent generation of distinct CD8+ memory T cell subsets. *Proc Natl Acad Sci U*  
710 *S A* 101, 5610-5615.

711 Joshi, N.S., Cui, W., Chandele, A., Lee, H.K., Urso, D.R., Hagman, J., Gapin, L., and Kaech,  
712 S.M. (2007). Inflammation directs memory precursor and short-lived effector CD8(+) T cell  
713 fates via the graded expression of T-bet transcription factor. *Immunity* 27, 281-295.

714 Joshi, N.S., Cui, W., Dominguez, C.X., Chen, J.H., Hand, T.W., and Kaech, S.M. (2011).  
715 Increased numbers of preexisting memory CD8 T cells and decreased T-bet expression can  
716 restrain terminal differentiation of secondary effector and memory CD8 T cells. *J Immunol*  
717 187, 4068-4076.

718 Julg, B., Williams, K.L., Reddy, S., Bishop, K., Qi, Y., Carrington, M., Goulder, P.J., Ndung'u,  
719 T., and Walker, B.D. (2010). Enhanced anti-HIV functional activity associated with Gag-  
720 specific CD8 T-cell responses. *J Virol* 84, 5540-5549.

721 Karlsson, I., Malleret, B., Brochard, P., Delache, B., Calvo, J., Le Grand, R., and Vaslin, B.  
722 (2007). Dynamics of T-cell responses and memory T cells during primary simian  
723 immunodeficiency virus infection in cynomolgus macaques. *J Virol* 81, 13456-13468.

724 Khanolkar, A., Fuller, M.J., and Zajac, A.J. (2004). CD4 T cell-dependent CD8 T cell  
725 maturation. *J Immunol* 172, 2834-2844.

726 Koup, R.A., Safrit, J.T., Cao, Y., Andrews, C.A., McLeod, G., Borkowsky, W., Farthing, C.,  
727 and Ho, D.D. (1994). Temporal association of cellular immune responses with the initial  
728 control of viremia in primary human immunodeficiency virus type 1 syndrome. *J Virol* 68,  
729 4650-4655.

730 Ladell, K., Hashimoto, M., Iglesias, M.C., Wilmann, P.G., McLaren, J.E., Gras, S., Chikata,  
731 T., Kuse, N., Fastenackels, S., Gostick, E., *et al.* (2013). A molecular basis for the control of  
732 preimmune escape variants by HIV-specific CD8<sup>+</sup> T cells. *Immunity* *38*, 425-436.

733 Lecuroux, C., Girault, I., Cheret, A., Versmisse, P., Nembot, G., Meyer, L., Rouzioux, C.,  
734 Pancino, G., Venet, A., Saez-Cirion, A., *et al.* (2013). CD8 T-cells from most HIV-infected  
735 patients lack ex vivo HIV-suppressive capacity during acute and early infection. *PLoS One* *8*,  
736 e59767.

737 Lecuroux, C., Saez-Cirion, A., Girault, I., Versmisse, P., Boufassa, F., Avettand-Fenoel, V.,  
738 Rouzioux, C., Meyer, L., Pancino, G., Lambotte, O., *et al.* (2014). Both HLA-B\*57 and  
739 plasma HIV RNA levels contribute to the HIV-specific CD8<sup>+</sup> T cell response in HIV  
740 controllers. *J Virol* *88*, 176-187.

741 Leong, Y.A., Chen, Y., Ong, H.S., Wu, D., Man, K., Deleage, C., Minnich, M., Meckiff, B.J.,  
742 Wei, Y., Hou, Z., *et al.* (2016). CXCR5(+) follicular cytotoxic T cells control viral infection in B  
743 cell follicles. *Nat Immunol* *17*, 1187-1196.

744 Lima, N.S., Takata, H., Huang, S.H., Haregot, A., Mitchell, J., Blackmore, S., Garland, A., Sy,  
745 A., Cartwright, P., Routy, J.P., *et al.* (2020). CTL Clonotypes with Higher TCR Affinity Have  
746 Better Ability to Reduce the HIV Latent Reservoir. *J Immunol*.

747 Liu, J., Keele, B.F., Li, H., Keating, S., Norris, P.J., Carville, A., Mansfield, K.G., Tomaras,  
748 G.D., Haynes, B.F., Kolodkin-Gal, D., *et al.* (2010). Low-dose mucosal simian  
749 immunodeficiency virus infection restricts early replication kinetics and transmitted virus  
750 variants in rhesus monkeys. *J Virol* *84*, 10406-10412.

751 Luxenburger, H., Neumann-Haefelin, C., Thimme, R., and Boettler, T. (2018). HCV-Specific  
752 T Cell Responses During and After Chronic HCV Infection. *Viruses* *10*.

753 Madelain, V., Passaes, C., Millet, A., Avettand-Fenoel, V., Djidjou-Demasse, R., Dereuddre-  
754 Bosquet, N., Le Grand, R., Rouzioux, C., Vaslin, B., Saez-Cirion, A., *et al.* (2020). Modeling  
755 SIV kinetics supports that cytotoxic response drives natural control and unravels  
756 heterogeneous populations of infected cells. *bioRxiv*, 2020.2001.2019.911594.

757 Mannioui, A., Bourry, O., Sellier, P., Delache, B., Brochard, P., Andrieu, T., Vaslin, B.,  
758 Karlsson, I., Roques, P., and Le Grand, R. (2009). Dynamics of viral replication in blood and  
759 lymphoid tissues during SIVmac251 infection of macaques. *Retrovirology* *6*, 106.

760 Martin, M.P., Gao, X., Lee, J.H., Nelson, G.W., Detels, R., Goedert, J.J., Buchbinder, S.,  
761 Hoots, K., Vlahov, D., Trowsdale, J., *et al.* (2002). Epistatic interaction between KIR3DS1  
762 and HLA-B delays the progression to AIDS. *Nat Genet* *31*, 429-434.

763 McBrien, J.B., Kumar, N.A., and Silvestri, G. (2018). Mechanisms of CD8(+) T cell-mediated  
764 suppression of HIV/SIV replication. *Eur J Immunol* *48*, 898-914.

765 Mee, E.T., Berry, N., Ham, C., Sauermann, U., Maggiorella, M.T., Martinon, F., Verschoor,  
766 E.J., Heeney, J.L., Le Grand, R., Titti, F., *et al.* (2009). Mhc haplotype H6 is associated with  
767 sustained control of SIVmac251 infection in Mauritian cynomolgus macaques.  
768 *Immunogenetics* *61*, 327-339.

769 Migueles, S.A., Laborico, A.C., Shupert, W.L., Sabbaghian, M.S., Rabin, R., Hallahan, C.W.,  
770 Van Baarle, D., Kostense, S., Miedema, F., McLaughlin, M., *et al.* (2002). HIV-specific CD8<sup>+</sup>  
771 T cell proliferation is coupled to perforin expression and is maintained in nonprogressors. *Nat*  
772 *Immunol* *3*, 1061-1068.

773 Migueles, S.A., Osborne, C.M., Royce, C., Compton, A.A., Joshi, R.P., Weeks, K.A., Rood,  
774 J.E., Berkley, A.M., Sacha, J.B., Cogliano-Shutta, N.A., *et al.* (2008). Lytic granule loading of  
775 CD8<sup>+</sup> T cells is required for HIV-infected cell elimination associated with immune control.  
776 *Immunity* *29*, 1009-1021.

777 Migueles, S.A., Sabbaghian, M.S., Shupert, W.L., Bettinotti, M.P., Marincola, F.M., Martino,  
778 L., Hallahan, C.W., Selig, S.M., Schwartz, D., Sullivan, J., *et al.* (2000). HLA B\*5701 is highly  
779 associated with restriction of virus replication in a subgroup of HIV-infected long term  
780 nonprogressors. *Proc Natl Acad Sci U S A* *97*, 2709-2714.

781 Ndhlovu, Z.M., Kanya, P., Mewalal, N., Klooverpris, H.N., Nkosi, T., Pretorius, K., Laher, F.,  
782 Ogunshola, F., Chopera, D., Shekhar, K., *et al.* (2015). Magnitude and Kinetics of CD8<sup>+</sup> T  
783 Cell Activation during Hyperacute HIV Infection Impact Viral Set Point. *Immunity* *43*, 591-604.

784 Noel, N., Pena, R., David, A., Avettand-Fenoel, V., Erkizia, I., Jimenez, E., Lecuroux, C.,  
785 Rouzioux, C., Boufassa, F., Pancino, G., *et al.* (2016). Long-Term Spontaneous Control of  
786 HIV-1 Is Related to Low Frequency of Infected Cells and Inefficient Viral Reactivation. *J Virol*  
787 *90*, 6148-6158.

788 O'Connor, D.H., Allen, T.M., Vogel, T.U., Jing, P., DeSouza, I.P., Dodds, E., Dunphy, E.J.,  
789 Melsaether, C., Mothe, B., Yamamoto, H., *et al.* (2002). Acute phase cytotoxic T lymphocyte  
790 escape is a hallmark of simian immunodeficiency virus infection. *Nat Med* *8*, 493-499.

791 O'Connor, S.L., Lhost, J.J., Becker, E.A., Detmer, A.M., Johnson, R.C., Macnair, C.E.,  
792 Wiseman, R.W., Karl, J.A., Greene, J.M., Burwitz, B.J., *et al.* (2010). MHC heterozygote  
793 advantage in simian immunodeficiency virus-infected Mauritian cynomolgus macaques. *Sci*  
794 *Transl Med* *2*, 22ra18.

795 Ozga, A.J., Moalli, F., Abe, J., Swoger, J., Sharpe, J., Zehn, D., Kreutzfeldt, M., Merkler, D.,  
796 Ripoll, J., and Stein, J.V. (2016). pMHC affinity controls duration of CD8+ T cell-DC  
797 interactions and imprints timing of effector differentiation versus expansion. *J Exp Med* *213*,  
798 2811-2829.

799 Paley, M.A., Kroy, D.C., Odorizzi, P.M., Johnnidis, J.B., Dolfi, D.V., Barnett, B.E., Bikoff,  
800 E.K., Robertson, E.J., Lauer, G.M., Reiner, S.L., *et al.* (2012). Progenitor and terminal  
801 subsets of CD8+ T cells cooperate to contain chronic viral infection. *Science* *338*, 1220-1225.

802 Pereyra, F., Addo, M.M., Kaufmann, D.E., Liu, Y., Miura, T., Rathod, A., Baker, B., Trocha,  
803 A., Rosenberg, R., Mackey, E., *et al.* (2008). Genetic and immunologic heterogeneity among  
804 persons who control HIV infection in the absence of therapy. *J Infect Dis* *197*, 563-571.

805 Petrovas, C., Casazza, J.P., Brenchley, J.M., Price, D.A., Gostick, E., Adams, W.C.,  
806 Precopio, M.L., Schacker, T., Roederer, M., Douek, D.C., *et al.* (2006). PD-1 is a regulator of  
807 virus-specific CD8+ T cell survival in HIV infection. *J Exp Med* *203*, 2281-2292.

808 Petrovas, C., Price, D.A., Mattapallil, J., Ambrozak, D.R., Geldmacher, C., Cecchinato, V.,  
809 Vaccari, M., Tryniszewska, E., Gostick, E., Roederer, M., *et al.* (2007). SIV-specific CD8+ T  
810 cells express high levels of PD1 and cytokines but have impaired proliferative capacity in  
811 acute and chronic SIVmac251 infection. *Blood* *110*, 928-936.

812 Picker, L.J. (2014). Are effector memory T cells the key to an effective HIV/AIDS vaccine?  
813 *EMBO Rep* *15*, 820-821.

814 Price, D.A., Brenchley, J.M., Ruff, L.E., Betts, M.R., Hill, B.J., Roederer, M., Koup, R.A.,  
815 Migueles, S.A., Gostick, E., Wooldridge, L., *et al.* (2005). Avidity for antigen shapes clonal  
816 dominance in CD8+ T cell populations specific for persistent DNA viruses. *J Exp Med* *202*,  
817 1349-1361.

818 Price, D.A., Goulder, P.J., Klenerman, P., Sewell, A.K., Easterbrook, P.J., Troop, M.,  
819 Bangham, C.R., and Phillips, R.E. (1997). Positive selection of HIV-1 cytotoxic T lymphocyte  
820 escape variants during primary infection. *Proc Natl Acad Sci U S A* *94*, 1890-1895.

821 Putkonen, P., Warstedt, K., Thorstensson, R., Benthin, R., Albert, J., Lundgren, B., Oberg,  
822 B., Norrby, E., and Biberfeld, G. (1989). Experimental infection of cynomolgus monkeys  
823 (*Macaca fascicularis*) with simian immunodeficiency virus (SIVsm). *J Acquir Immune Defic*  
824 *Syndr* *2*, 359-365.

825 Rao, R.R., Li, Q., Gubbels Bupp, M.R., and Shrikant, P.A. (2012). Transcription factor Foxo1  
826 represses T-bet-mediated effector functions and promotes memory CD8(+) T cell  
827 differentiation. *Immunity* *36*, 374-387.

828 Reuter, M.A., Del Rio Estrada, P.M., Buggert, M., Petrovas, C., Ferrando-Martinez, S.,  
829 Nguyen, S., Sada Japp, A., Ablanado-Terrazas, Y., Rivero-Arrieta, A., Kuri-Cervantes, L., *et*  
830 *al.* (2017). HIV-Specific CD8(+) T Cells Exhibit Reduced and Differentially Regulated  
831 Cytolytic Activity in Lymphoid Tissue. *Cell Rep* *21*, 3458-3470.

832 Rutishauser, R.L., Deguit, C.D.T., Hiatt, J., Blaeschke, F., Roth, T.L., Wang, L., Raymond,  
833 K., Starke, C.E., Mudd, J.C., Chen, W., *et al.* (2020). TCF-1 regulates the stem-like memory  
834 potential of HIV-specific CD8+ T cells in elite controllers. *bioRxiv*, 2020.2001.2007.894535.

835 Saez-Cirion, A., Bacchus, C., Hocqueloux, L., Avettand-Fenoel, V., Girault, I., Lecuroux, C.,  
836 Potard, V., Versmisse, P., Melard, A., Prazuck, T., *et al.* (2013). Post-treatment HIV-1  
837 controllers with a long-term virological remission after the interruption of early initiated  
838 antiretroviral therapy ANRS VISCONTI Study. *PLoS Pathog* *9*, e1003211.

839 Saez-Cirion, A., Lacabaratz, C., Lambotte, O., Versmisse, P., Urrutia, A., Boufassa, F.,  
840 Barre-Sinoussi, F., Delfraissy, J.F., Sinet, M., Pancino, G., *et al.* (2007). HIV controllers  
841 exhibit potent CD8 T cell capacity to suppress HIV infection ex vivo and peculiar cytotoxic T  
842 lymphocyte activation phenotype. *Proc Natl Acad Sci U S A* *104*, 6776-6781.

843 Saez-Cirion, A., and Pancino, G. (2013). HIV controllers: a genetically determined or  
844 inducible phenotype? *Immunol Rev* *254*, 281-294.

845 Saez-Cirion, A., Shin, S.Y., Versmisse, P., Barre-Sinoussi, F., and Pancino, G. (2010). Ex  
846 vivo T cell-based HIV suppression assay to evaluate HIV-specific CD8+ T-cell responses.  
847 *Nat Protoc* *5*, 1033-1041.

848 Saez-Cirion, A., Sinet, M., Shin, S.Y., Urrutia, A., Versmisse, P., Lacabaratz, C., Boufassa,  
849 F., Avettand-Fenoel, V., Rouzioux, C., Delfraissy, J.F., *et al.* (2009). Heterogeneity in HIV  
850 suppression by CD8 T cells from HIV controllers: association with Gag-specific CD8 T cell  
851 responses. *J Immunol* *182*, 7828-7837.

852 Schluns, K.S., Kieper, W.C., Jameson, S.C., and Lefrancois, L. (2000). Interleukin-7  
853 mediates the homeostasis of naive and memory CD8 T cells in vivo. *Nat Immunol* *1*, 426-  
854 432.

855 Simonetta, F., Hua, S., Lecuroux, C., Gerard, S., Boufassa, F., Saez-Cirion, A., Pancino, G.,  
856 Goujard, C., Lambotte, O., Venet, A., *et al.* (2014). High eomesodermin expression among  
857 CD57+ CD8+ T cells identifies a CD8+ T cell subset associated with viral control during  
858 chronic human immunodeficiency virus infection. *J Virol* *88*, 11861-11871.

859 Snell, L.M., MacLeod, B.L., Law, J.C., Osokine, I., Elsaesser, H.J., Hezaveh, K., Dickson,  
860 R.J., Gavin, M.A., Guidos, C.J., McGaha, T.L., *et al.* (2018). CD8(+) T Cell Priming in  
861 Established Chronic Viral Infection Preferentially Directs Differentiation of Memory-like Cells  
862 for Sustained Immunity. *Immunity* *49*, 678-694 e675.

863 Sullivan, B.M., Juedes, A., Szabo, S.J., von Herrath, M., and Glimcher, L.H. (2003). Antigen-  
864 driven effector CD8 T cell function regulated by T-bet. *Proc Natl Acad Sci U S A* *100*, 15818-  
865 15823.

866 Szabo, S.J., Sullivan, B.M., Stemmann, C., Satoskar, A.R., Sleckman, B.P., and Glimcher,  
867 L.H. (2002). Distinct effects of T-bet in TH1 lineage commitment and IFN-gamma production  
868 in CD4 and CD8 T cells. *Science* *295*, 338-342.

869 Takata, H., Buranapraditkun, S., Kessing, C., Fletcher, J.L., Muir, R., Tardif, V., Cartwright,  
870 P., Vandergeeten, C., Bakeman, W., Nichols, C.N., *et al.* (2017). Delayed differentiation of  
871 potent effector CD8(+) T cells reducing viremia and reservoir seeding in acute HIV infection.  
872 *Sci Transl Med* *9*.

873 Takemoto, N., Intlekofer, A.M., Northrup, J.T., Wherry, E.J., and Reiner, S.L. (2006). Cutting  
874 Edge: IL-12 inversely regulates T-bet and eomesodermin expression during pathogen-  
875 induced CD8+ T cell differentiation. *J Immunol* *177*, 7515-7519.

876 Tansiri, Y., Rowland-Jones, S.L., Ananworanich, J., and Hansasuta, P. (2015). Clinical  
877 outcome of HIV viraemic controllers and noncontrollers with normal CD4 counts is  
878 exclusively determined by antigen-specific CD8+ T-cell-mediated HIV suppression. *PLoS*  
879 *One* *10*, e0118871.

880 Trautmann, L., Janbazian, L., Chomont, N., Said, E.A., Gimmig, S., Bessette, B., Boulassel,  
881 M.R., Delwart, E., Sepulveda, H., Balderas, R.S., *et al.* (2006). Upregulation of PD-1  
882 expression on HIV-specific CD8+ T cells leads to reversible immune dysfunction. *Nat Med*  
883 *12*, 1198-1202.

884 Trautmann, L., Mbitikon-Kobo, F.M., Goulet, J.P., Peretz, Y., Shi, Y., Van Grevenynghe, J.,  
885 Procopio, F.A., Boulassel, M.R., Routy, J.P., Chomont, N., *et al.* (2012). Profound metabolic,  
886 functional, and cytolytic differences characterize HIV-specific CD8 T cells in primary and  
887 chronic HIV infection. *Blood* *120*, 3466-3477.

888 Utzschneider, D.T., Charmoy, M., Chennupati, V., Pousse, L., Ferreira, D.P., Calderon-  
889 Copete, S., Danilo, M., Alfei, F., Hofmann, M., Wieland, D., *et al.* (2016). T Cell Factor 1-  
890 Expressing Memory-like CD8(+) T Cells Sustain the Immune Response to Chronic Viral  
891 Infections. *Immunity* *45*, 415-427.

892 van den Berg, S.P.H., Pardieck, I.N., Lanfermeijer, J., Sauce, D., Klenerman, P., van Baarle,  
893 D., and Arens, R. (2019). The hallmarks of CMV-specific CD8 T-cell differentiation. *Med*  
894 *Microbiol Immunol* 208, 365-373.  
895 Veazey, R.S., Gauduin, M.C., Mansfield, K.G., Tham, I.C., Altman, J.D., Lifson, J.D.,  
896 Lackner, A.A., and Johnson, R.P. (2001). Emergence and kinetics of simian  
897 immunodeficiency virus-specific CD8(+) T cells in the intestines of macaques during primary  
898 infection. *J Virol* 75, 10515-10519.  
899 Walker, B., and McMichael, A. (2012). The T-cell response to HIV. *Cold Spring Harb*  
900 *Perspect Med* 2.  
901 Ye, B., Liu, X., Li, X., Kong, H., Tian, L., and Chen, Y. (2015). T-cell exhaustion in chronic  
902 hepatitis B infection: current knowledge and clinical significance. *Cell Death Dis* 6, e1694.  
903 Zhou, X., Yu, S., Zhao, D.M., Harty, J.T., Badovinac, V.P., and Xue, H.H. (2010).  
904 Differentiation and persistence of memory CD8(+) T cells depend on T cell factor 1. *Immunity*  
905 33, 229-240.  
906 Zimmerli, S.C., Harari, A., Cellerai, C., Vallelian, F., Bart, P.A., and Pantaleo, G. (2005). HIV-  
907 1-specific IFN-gamma/IL-2-secreting CD8 T cells support CD4-independent proliferation of  
908 HIV-1-specific CD8 T cells. *Proc Natl Acad Sci U S A* 102, 7239-7244.  
909

910

911 **FIGURE LEGENDS**

912 **Figure 1. SIV controllers are characterized by early preservation of lymph nodes and**  
913 **progressive decline in the frequency of SIV-carrying cells.** Plasma VL kinetics (A),  
914 longitudinal evolution of CD4<sup>+</sup> T-cell counts in blood (B), in rectal mucosa (D), and peripheral  
915 lymph nodes (E) in SIV controllers (SICs, grey) and viremic CyMs (VIRs, red). Results are  
916 shown as fold-change in absolute CD4<sup>+</sup> T-cell counts relative to baseline in blood and as fold-  
917 change in percent frequencies of CD4<sup>+</sup> T-cells among CD3<sup>+</sup> lymphocytes relative to baseline  
918 in RBs and pLNs. (F) Percent frequencies of CD4<sup>+</sup> T-cells among CD3<sup>+</sup> lymphocytes in bone  
919 marrow, spleen, peripheral and mesenteric LNs, and colon mucosa at euthanasia. Kinetics of  
920 SIV-DNA levels in blood (C), in RBs (G), and pLNs (H). (I) Levels of SIV-DNA in bone marrow,  
921 spleen, peripheral and mesenteric lymph nodes, and colon at euthanasia. Results are  
922 expressed as copies SIV-DNA/million CD4<sup>+</sup> T-cells. Median and interquartile range are shown  
923 (n=12 SICs; n=4 VIRs). \*p < 0.05, \*\*p < 0.01; Mann-Whitney U-test.

924

925 **Figure 2. The dynamics of CD8<sup>+</sup> T-cell expansion and activation do not predict control of**  
926 **SIV. (A–C) Evolution of Ki-67<sup>+</sup> CD8<sup>+</sup> T cells in blood (A), peripheral lymph nodes (B), and**  
927 **rectal mucosa (C) in SIV controllers (grey) and viremics (red). (D–F) Evolution of CD38<sup>+</sup> HLA-**  
928 **DR<sup>+</sup> CD8<sup>+</sup> T cells in blood (D), pLNs (E), and RB (F). Median and interquartile range are**  
929 **shown. Vertical dashed lines indicate peak VLs. \*p < 0.05, \*\*p < 0.01; Mann-Whitney U-test.**

930

931 **Figure 3. SIV-specific CD8<sup>+</sup> T-cell frequencies do not predict control of SIV. (A) TNF $\alpha$**   
932 **production by SIV-specific CD8<sup>+</sup> T-cells in blood and pLNs over the course of infection and in**  
933 **bone marrow, spleen, and MLNs at euthanasia in SICs (grey) and VIRs (red). Results are**  
934 **shown as percent frequencies among CD8<sup>+</sup> T-cells. Median and interquartile range are**

935 shown (n=12 SICs; n=4 VIRs). **(B)** Functional profiles of SIV-specific CD8<sup>+</sup> T-cells in blood and  
936 pLNs over the course of infection and in bone marrow, spleen, and MLNs at euthanasia.  
937 Doughnut charts show median percent frequencies of SIV-specific CD8<sup>+</sup> T-cells expressing  
938 IFN $\gamma$ , TNF $\alpha$ , IL-2, and/or CD107a (n=12 SICs; n=4 VIRs). Colors indicate number of  
939 simultaneous functions (blue, 1; green, 2; yellow, 3; red, 4). \*p < 0.05; Mann-Whitney U-test.  
940

941 **Figure 4. Progressive acquisition of CD8<sup>+</sup> T-cell-mediated SIV-suppressive activity is**  
942 **associated with control of SIV. (A)** CD8<sup>+</sup> T-cell-mediated SIV-suppressive activity in blood  
943 and pLNs over the course of infection and in bone marrow, spleen, and MLNs at euthanasia  
944 in SICs (grey) and VIRs (red). Results are shown as log p27 decrease in the presence of CD8<sup>+</sup>  
945 T-cells. \*p < 0.05, \*\*p < 0.01; Mann-Whitney U-test. **(B)** Spearman correlations between  
946 CD8<sup>+</sup> T-cell-mediated SIV-suppressive activity (upper panel) or TNF $\alpha$  production by SIV-  
947 specific CD8<sup>+</sup> T-cells (bottom panel) on day 15 *p.i.* with plasma VL on day 15 *p.i.* **(C)**  
948 Spearman correlations between CD8<sup>+</sup> T-cell-mediated SIV-suppressive activity (upper panel)  
949 or TNF $\alpha$  production by SIV-specific CD8<sup>+</sup> T-cells (bottom panel) at euthanasia with plasma VL  
950 at euthanasia. **(D)** Spearman correlations between area under the curve (AUC) for plasma VL  
951 and AUC for CD8<sup>+</sup> T-cell-mediated SIV-suppressive activity (orange) and between AUC for  
952 plasma VL and AUC for TNF $\alpha$  production by SIV-specific CD8<sup>+</sup> T-cells (blue). AUC for plasma  
953 VL, TNF $\alpha$  production and CD8<sup>+</sup> T-cell antiviral activities were calculated using the sequential  
954 values obtained throughout the duration of our study in the blood of the infected animals  
955 (Figure S7). **(E)** Side by side comparison of the longitudinal kinetics of TNF $\alpha$  production by  
956 SIV-specific CD8<sup>+</sup> T-cells in blood shown in figure 2A (blue) and CD8<sup>+</sup> T-cell-mediated SIV-  
957 suppressive activity in blood shown in figure 3A (orange) in SICs (left panel) and VIRs (right  
958 panel). Median and interquartile range are shown (n=12 SICs; n=4 VIRs).

959

960 **Figure 5. SIV controllers maintain higher frequencies of SIV-specific central memory CD8<sup>+</sup>**  
961 **T-cells during chronic infection than viremic CyMs. (A)** Bar charts showing median percent  
962 frequencies of SIV-specific CD8<sup>+</sup> T-cells in each phenotypically-defined subset in SICs and  
963 VIRs. Light blue, central memory (CM); green, transitional memory (TM); yellow, effector  
964 memory (EM); red, effector (Eff). **(B)** Evolution of CM, TM, EM, and Eff SIV-specific CD8<sup>+</sup> T-  
965 cells. Results are shown as percent frequencies of tetramer-binding CD8<sup>+</sup> T-cells. Median and  
966 interquartile range are shown (n=12 SICs; n=4 VIRs). \*p < 0.05; Mann-Whitney U-test.

967

968 **Figure 6. Altered maturation of central memory SIV-specific CD8<sup>+</sup> T-cells in viremic CyMs.**  
969 **(A)** Dynamics of T-bet (left panels) and CD127 expression (right panels) among SIV-specific  
970 CD8<sup>+</sup> T-cells in SICs (n=12) (grey) and VIRs (n=4) (red). **(B)** Dynamics of T-bet (left) and CD127  
971 expression among central memory, transitional memory, effector memory, and effector SIV-  
972 specific CD8<sup>+</sup> T-cells. \*p < 0.05, \*\*p < 0.01; Mann-Whitney U-test.

973

974 **Figure 7. Skewed maturation of central memory SIV-specific CD8<sup>+</sup> T-cells is associated with**  
975 **defective acquisition of SIV-suppressive activity.** Spearman correlations between CD127<sup>+</sup>  
976 SIV-specific CD8<sup>+</sup> T-cell frequencies and viral loads **(A)** and CD8<sup>+</sup> T-cell-mediated SIV-  
977 suppressive activity **(B)** during acute (left panel) and chronic infection (right panel).  
978 Spearman correlations between T-bet<sup>+</sup> CD127<sup>-</sup> SIV-specific CD8<sup>+</sup> T-cell frequencies **(C)** or T-  
979 bet expression levels in central memory SIV-specific CD8<sup>+</sup> T-cells **(D)** and CD8<sup>+</sup> T-cell-  
980 mediated SIV-suppressive activity during acute (left panel) and chronic infection (right  
981 panel). Grey symbols, SICs (n=12); red symbols, VIRs (n=4). **(E)** Expression levels of TCF-1  
982 among total, central memory, transitional memory, effector memory, and effector SIV-

983 specific CD8<sup>+</sup> T-cells (left panel); and proportion of SIV-specific CD8<sup>+</sup> T-cells coexpressing TCF-  
984 1, CCR7 and CXCR5 (right panel). \*\*p < 0.01; Mann-Whitney U-test.

985 **STAR METHODS**

986 **RESOURCE AVAILABILITY**

987 ***Lead Contact***

988 Further information and requests for resources and reagents should be directed to the Lead  
989 Contact, Asier Saez-Cirion (asier.saez-cirion@pasteur.fr). Request for biological resources  
990 will be fulfilled based on availability and upon the establishment of a MTA.

991 ***Materials Availability***

992 This study did not generate new unique reagents.

993 ***Data and Code Availability***

994 This study did not generate/analyze datasets/code.

995

996 **EXPERIMENTAL MODEL AND SUBJECT DETAILS**

997 ***Ethical statement***

998 CyMs were imported from Mauritius and housed in facilities at the *Commissariat à l'Energie*  
999 *Atomique et aux Energies Alternatives* (CEA, Fontenay-aux-Roses, France). All non-human  
1000 primate studies at the CEA are conducted in accordance with French National Regulations  
1001 under the supervision of National Veterinary Inspectors (CEA Permit Number A 92-03-02).  
1002 The CEA complies with the Standards for Human Care and Use of Laboratory Animals of the  
1003 Office for Laboratory Animal Welfare under Assurance Number #A5826-01. All experimental  
1004 procedures were conducted according to European Directive 2010/63 (Recommendation  
1005 Number 9). The SIC and pVISCONTI studies were approved and accredited under statements  
1006 A13-005 and A15-035 from the "*Comité d'Ethique en Expérimentation Animale du CEA*",  
1007 registered and authorized under Number 44 and Number 2453-2015102713323361v2 by the  
1008 French Ministry of Education and Research. CyMs were studied with veterinary guidance,  
1009 housed in adjoining individual cages allowing social interactions, and maintained under  
1010 controlled conditions with respect to humidity, temperature, and light (12 hr light/12 hr dark  
1011 cycles). Water was available *ad libitum*. Animals were monitored and fed with commercial

1012 monkey chow and fruit once or twice daily by trained personnel. Environmental enrichment  
1013 was provided in the form of toys, novel foodstuffs, and music under the supervision of the  
1014 CEA Animal Welfare Body. Experimental procedures (animal handling, viral inoculations, and  
1015 samplings) were conducted after sedation with ketamine chlorhydrate (Imalgene 1000®, 10  
1016 mg/kg, *i.v.*, Merial). Tissues were collected at necropsy. Animals were sedated with ketamine  
1017 chlorhydrate and euthanized humanely with sodium pentobarbital (Doléthal, 180 mg/kg, *i.v.*,  
1018 Laboratoire Vetoquinol).

1019

### 1020 ***Animals and SIV infection***

1021 A total of 16 healthy adult male CyMs (median age = 6.8 years at inclusion, IQR = 5.8–7.2)  
1022 were selected for this study on the basis of MHC haplotype (M6<sup>+</sup>, n = 6; M6<sup>-</sup>, n = 10) (34).  
1023 CyMs were inoculated *i.r.* with either 5AID<sub>50</sub> or 50AID<sub>50</sub> of uncloned SIVmac251 (A.M.  
1024 Aubertin, Université Louis Pasteur, Strasbourg, France). The following experimental groups  
1025 were studied: (i) M6<sup>-</sup> CyMs inoculated *i.r.* with 5AID<sub>50</sub> (non-M6 5AID<sub>50</sub>, n = 4); (ii) M6<sup>+</sup> CyMs  
1026 inoculated *i.r.* with 50AID<sub>50</sub> (M6 50AID<sub>50</sub>, n = 6); and (iii) M6<sup>-</sup> CyMs inoculated *i.r.* with  
1027 50AID<sub>50</sub> (non-M6 50AID<sub>50</sub>, n = 6). Animals were monitored for 18 months after infection.

1028

1029 The outcome of infection generally matched expectations based on previous studies for each  
1030 experimental group (Figure S7A, Table S4). Only one M6<sup>+</sup> CyM (31041) was unable to control  
1031 viremia below 400 copies/mL. This animal was homozygous for MHC class I (Table S1), which  
1032 intrinsically limits immune control of HIV/SIV (Carrington et al., 1999; O'Connor et al., 2010).  
1033 The dynamics of viral replication during acute infection were very similar in the three  
1034 experimental groups, with peak VLs of 5.9, 6.4, and 6.3 log SIV-RNA copies/mL of plasma on

1035 day 14 *p.i.* for non-M6 5AID<sub>50</sub>, M6 50AID<sub>50</sub>, and non-M6 50AID<sub>50</sub> CyMs, respectively (Table  
1036 S4).

1037

1038 CyMs in the pVISCONTI study (median age = 5 years at inclusion, IQR = 4.1–5.3) were  
1039 inoculated *i.v.* with 1000 AID<sub>50</sub> of uncloned SIVmac251. None of these animals carried the M6  
1040 haplotype. An antiretroviral regimen containing emtricitabine (FTC, 40 mg/kg, Gilead),  
1041 dolutegravir (DTG, 2.5 mg/kg, ViiV Healthcare), and the tenofovir prodrug tenofovir-  
1042 disoproxil-fumarate (TDF, 5.1 mg/kg, Gilead), coformulated as a once daily subcutaneous  
1043 injection, was initiated on day 28 *p.i.* in 6 animals.

1044

## 1045 **METHOD DETAILS**

### 1046 ***Blood collection and processing***

1047 Peripheral blood was collected by venous puncture into Vacutainer Plus Plastic K3EDTA  
1048 Tubes or Vacutainer CPT Mononuclear Cell Preparation Tubes with Sodium Heparin (BD  
1049 Biosciences). Complete blood counts were monitored at all time points from the Vacutainer  
1050 Plus Plastic K3EDTA Tubes. Plasma was isolated from Vacutainer Plus Plastic K3EDTA Tubes  
1051 by centrifugation for 10 min at 1,500 g and stored at –80°C. Peripheral blood mononuclear  
1052 cells (PBMCs) were isolated from Vacutainer CPT Mononuclear Cell Preparation Tubes with  
1053 Sodium Heparin according to manufacturer’s instructions (BD Biosciences), and red blood  
1054 cells were lysed in ACK (0.15 M NH<sub>4</sub>Cl, 10 mM KHCO<sub>3</sub>, 0.1 mM EDTA, pH 7.4).

1055

### 1056 ***Tissue collection and processing***

1057 Axillary or inguinal LNs (PLNs), RBs, and broncho-alveolar lavages (BALs) were collected  
1058 longitudinally from each animal at the indicated time points. Bone marrow, spleen,

1059 mesenteric lymph nodes (MLNs), duodenum, jejunum, ileum, and colon were collected at  
1060 necropsy. Tissue samples were snap-frozen in liquid nitrogen for storage at  $-80^{\circ}\text{C}$  or  
1061 collected in RPMI medium at  $2-8^{\circ}\text{C}$ . A complete PLN group was collected at each time point.  
1062 LN cells were isolated into RPMI medium via mechanical disruption using a gentleMACS  
1063 Dissociator (Miltenyi Biotec). The cell suspension was filtered ( $70\ \mu\text{m}$ ), and red blood cells  
1064 were lysed in ACK. RB lymphocytes were obtained from approximately  $4\ \text{mm}^2$  of rectal  
1065 mucosa. Colonic lymphocytes were obtained from mucosa taken from approximately 10 cm  
1066 of tissue. RBs and colonic tissue were washed extensively in R10 medium (RPMI medium  
1067 supplemented with 10% fetal calf serum and penicillin/neomycin/streptomycin), and then  
1068 digested for 45 min with collagenase II prior to mechanical disruption. Lymphocytes were  
1069 isolated over a Percoll 67/44 gradient (Sigma-Aldrich). Bone marrow cells were purified using  
1070 Lymphocyte Separation Medium (Lonza Bioscience) diluted to 90% in DPBS, centrifuged for  
1071 20 min at 350 g, and separated from red cells in ACK. Spleen cells were processed via  
1072 mechanical disruption in RPMI medium using a gentleMACS Dissociator (Miltenyi Biotec),  
1073 purified as described for bone marrow cells, and separated from red cells in ACK. T-cell  
1074 activation and proliferation assays and measurements of SIV-suppressive activity were  
1075 performed using freshly isolated cells, and intracellular cytokine assays and tetramer stains  
1076 were performed using cells frozen viably at  $-80^{\circ}\text{C}$ .

1077

#### 1078 ***Quantification of plasma viral load***

1079 Plasma viremia was monitored longitudinally in all animals using quantitative RT-PCR with a  
1080 limit of detection of 12.3 copies/mL. Viral RNA was prepared from  $100\ \mu\text{L}$  of cell-free plasma.  
1081 Quantitative RT-PCR was performed using a SuperScript III Platinum One-Step qRT-PCR Kit  
1082 (Thermo Fisher Scientific) with a CFX96 Touch Real-Time PCR Detection System (Bio-Rad).

1083 Each tube contained 12.5  $\mu\text{L}$  of 2X reaction mixture, 0.5  $\mu\text{L}$  of RNaseOUT (40 U/ $\mu\text{L}$ ), 0.5  $\mu\text{L}$  of  
1084 Superscript III Reverse Transcriptase/Platinum Taq DNA Polymerase, 1  $\mu\text{L}$  of each primer  
1085 (125  $\mu\text{M}$ ), 0.5  $\mu\text{L}$  of the fluorogenic probe (135  $\mu\text{M}$ ), and 10  $\mu\text{L}$  of eluted RNA. Primer/probe  
1086 sequences were designed to amplify a region of SIVmac251 *gag*. The forward (F) primer  
1087 sequence was 5'-GCAGAGGAGGAAATTACCCAGTAC-3' (24 bp), and the reverse (R) primer  
1088 sequence was 5'-CAATTTTACCCAGGCATTTAATGTT-3' (25 bp). The probe sequence was 5'-  
1089 FAM-TGTCCACCTGCCATTAAGCCCGA-BHQ1-3' (23 bp). This probe had a fluorescent reporter  
1090 dye, FAM (6-carboxyfluorescein), attached to its 5' end and a quencher, BHQ1 (Black Hole  
1091 Quencher 1), attached to its 3' end (TaqMan, Applied Biosystems). Samples were heated for  
1092 30 min at 56°C and 5 min at 95°C, followed by 50 thermocycles, each comprising 15 sec at  
1093 95°C and 1 min at 60°C.

1094

#### 1095 ***Quantification of SIV-DNA***

1096 Total DNA was extracted from purified CD14<sup>+</sup> alveolar macrophages, buffy coats, and snap-  
1097 frozen tissues. CD14<sup>+</sup> alveolar macrophages were purified magnetically via positive selection  
1098 using CD14 MicroBeads (Miltenyi Biotec). Purity was checked using flow cytometry (Figure  
1099 S1B). Snap-frozen tissues were mechanically disrupted using a MagNA Lyser (Roche  
1100 Diagnostics). DNA was extracted using a QIAamp DNA Blood Mini Kit (Qiagen). SIV-DNA was  
1101 quantified using an ultrasensitive quantitative real-time PCR. For blood samples, 150,000  
1102 cells were analyzed in each PCR. Sample limitations restricted input numbers to 20,000 cells  
1103 for BALs and 50,000 cells for RBs. All amplifications were performed over 2–4 replicates. The  
1104 cell line SIV1C, which contains 1 copy of SIV integrated/cell, was used as a standard for  
1105 quantification. A total of 1  $\mu\text{g}$  of DNA was considered to be equivalent to 150,000 cells.  
1106 Amplification was performed using primers and a probe located in the *gag* region. The *CCR5*

1107 gene was used to normalize results per million cells. Results were adjusted by the  
1108 frequencies of CD4<sup>+</sup> T-cells in blood and tissues, according to availability. The limit of  
1109 quantification was 2 copies/PCR. Primer and probe sequences were: SIV *gag* F: 5'-  
1110 GCAGAGGAGGAAATTACCCAGTAC-3'; SIV *gag* R: 5'-CAATTTTACCCAGGCATTTAATGTT-3'; SIV  
1111 *gag* probe: 5'-FAM-TGTCCACCTGCCATTAAGCCCGA-BHQ1-3'; *CCR5* F: an equimolar mix of 5'-  
1112 CAACATGCTGGTCGATCCTCAT-3' and 5'-CAACATACTGGTCGTCCTCATCC-3'; *CCR5* R: 5'-  
1113 CAGCATAGTGAGCCCAGAAG-3'; and *CCR5* probe: 5'-HEX-CTGACATCTACCTGCTCAACCTG-  
1114 BHQ1-3'.

1115

#### 1116 ***Viral reactivation in autologous CD4<sup>+</sup> T-cells***

1117 Autologous CD4<sup>+</sup> T-cells were purified magnetically from freshly isolated PBMCs using an  
1118 EasySep CD4 Positive Selection Kit with an automated RoboSep (StemCell Technologies).  
1119 Purified CD4<sup>+</sup> T-cells were stimulated for 3 days with concanavalin A (5µg/mL, Sigma-Aldrich)  
1120 in the presence of IL-2 (100 IU/mL, Miltenyi Biotec). Stimulated CD4<sup>+</sup> T-cells (10<sup>5</sup>) were  
1121 cultured in R10 medium containing IL-2 (100 IU/mL, Miltenyi Biotec). The production of SIV  
1122 p27 was measured in culture supernatants on day 7 using an SIV p27 Antigen ELISA Kit  
1123 (Zeptometrix).

1124

#### 1125 ***Measurement of T-cell activation and proliferation***

1126 T-cell activation and proliferation were assessed using fresh PBMCs and tissue cell  
1127 suspensions. Blood samples were treated with FACS Lysing Solution (BD Biosciences). Cells  
1128 were surface stained for CD3, CD4, CD8, CD38, CD45, CCR5, and HLA-DR,  
1129 fixed/permeabilized using a Cytofix/CytoPerm Kit (BD Biosciences), and stained  
1130 intracellularly for Ki-67. The following antibodies used were: anti-CD3-PE (clone SP34-2, BD

1131 Biosciences), anti-CD4–PerCP–Cy5.5 (clone L200, BD Biosciences), anti-CD8–BV650 (clone  
1132 RPA-T8, BioLegend), anti-CD38–FITC (clone AT-1, StemCell Technologies), anti-CD45–V500  
1133 (clone D058-1283, BD Biosciences), anti-CCR5–APC (clone 3A9, BD Biosciences), anti-HLA-  
1134 DR–APC–H7 (clone G46-6, BD Biosciences), and anti-Ki-67–AF700 (clone B56, BD  
1135 Biosciences). Data were acquired using an LSRII flow cytometer (BD Biosciences) and  
1136 analyzed with FlowJo software version 10 (Tree Star Inc.).

1137

### 1138 ***Intracellular cytokine staining***

1139 Frozen PBMCs, PLN cells, bone marrow cells, splenocytes, and MLN cells were thawed,  
1140 resuspended at  $1 \times 10^6$ /mL in R20 medium, and stored overnight at 37°C. Cells were then  
1141 stimulated with a pool of 24 optimal SIV peptides (8–10 amino acids, 2 µg/mL each, Table  
1142 S3) or with a pool of 125 overlapping SIV Gag 15mer peptides (SIVmac239 Gag Peptide Set  
1143 #12364, 2 µg/mL each, NIH AIDS Reagent Program) in the presence of anti-CD28 (1 µg/mL,  
1144 clone L293, BD Biosciences) and anti-CD49d (1 µg/mL, clone 9F10, BD Biosciences) and  
1145 stained with anti-CD107a (clone H4A3, BD Biosciences) for 30 min prior to the addition of  
1146 GolgiStop (1 µL/mL, BD Biosciences) and brefeldin A (BFA, 5 µg/mL, Sigma-Aldrich).  
1147 Costimulatory antibodies alone were used as a negative control, and concanavalin A (5  
1148 µg/mL, Sigma-Aldrich) was used as a positive control. Cells were incubated for a total of 6 hr.  
1149 After washing, cells were surface stained for CD3, CD4, and CD8, fixed/permeabilized using a  
1150 Cytofix/CytoPerm Kit (BD Biosciences), and stained intracellularly for IFN $\gamma$ , TNF $\alpha$ , and IL-2.  
1151 The following antibodies were used: anti-CD107a–V450 (clone H4A3, BD Biosciences), anti-  
1152 CD3–AF700 (clone SP34-2, BD Biosciences), anti-CD4–PerCP–Cy5.5 (clone L200, BD  
1153 Biosciences), anti-CD8–APC–Cy7 (clone RPA-T8, BD Biosciences), anti-IFN $\gamma$ –PE–Cy7 (clone  
1154 B27, BD Biosciences), anti-IL-2–PE (clone MQ1-17H12, BD Biosciences), and anti-TNF $\alpha$ –PE-

1155 CF594 (clone Mab11, BD Biosciences). Data were acquired using an LSRII flow cytometer (BD  
1156 Biosciences) and analyzed with FlowJo software version 10 (Tree Star Inc.). Results were  
1157 corrected for background by subtracting the negative (no peptide) control from the peptide  
1158 stimulated response. Negative responses were given an arbitrary value of 0.001.

1159

#### 1160 ***MHC class I tetramer staining***

1161 Biotinylated complexes of Nef RM9 (RPKVPLRTM)–Mafa A1\*063:02, Gag GW9  
1162 (GPRKPIKCW)–Mafa A1\*063:02, and Vpx GR9 (GEAFEWLNR)–Mafa B\*095:01 were produced  
1163 as described previously (Price et al., 2005). The corresponding tetramers were generated via  
1164 the stepwise addition of APC-conjugated streptavidin (Thermo Fisher Scientific). Frozen  
1165 PBMCs were stained with all tetramers simultaneously for 30 min at 37°C, washed, and  
1166 surface stained for CD3, CD4, CD8, CD14, CD20, CD27, CD45RA, CCR7, HLA-DR, and CD127.  
1167 Cells were then fixed/permeabilized using a Cytofix/CytoPerm Kit (BD Biosciences) and  
1168 stained for T-bet. The following antibodies were used: anti-CD3–AF700 (clone SP34-2, BD  
1169 Biosciences), anti-CD4–PerCP-Cy5.5 (clone L200, BD Biosciences), anti-CD8–APC-Cy7 (clone  
1170 RPA-T8, BD Biosciences), anti-CD14–BV786 (clone M5E2, BD Biosciences), anti-CD20–BV786  
1171 (clone L27, BD Biosciences), anti-CD27–PE (clone M-T271, BD Biosciences), anti-CD45RA–PE-  
1172 Cy7 (clone 5H9, BD Biosciences), anti-CCR7–PE-Dazzle594 (clone G043H7, BioLegend), anti-  
1173 HLA-DR–Pacific Blue (clone G46-6, BD Biosciences), anti-CD127–FITC (clone MB15-18C9,  
1174 Miltenyi Biotec), and anti-T-bet–BV711 (clone 4B10, BioLegend). Data were acquired using  
1175 an Arialll flow cytometer (BD Biosciences) and analyzed with FlowJo software version 10  
1176 (Tree Star Inc.). MFI stands for median fluorescence intensity.

1177

#### 1178 ***TCF-1 staining***

1179 Frozen splenocytes were stained with tetramers as described above, washed, and surface  
1180 stained for CD3, CD4, CD8, CD14, CD20, CD27, CD45RA, CCR7, and CXCR5. Cells were then  
1181 fixed/permeabilized using a Transcription Factor Buffer Set (BD Biosciences) and stained for  
1182 TCF-1. The following antibodies were used: anti-CD3–AF700 (clone SP34-2, BD Biosciences),  
1183 anti-CD4–PerCP-Cy5.5 (clone L200, BD Biosciences), anti-CD8–APC-Cy7 (clone RPA-T8, BD  
1184 Biosciences), anti-CD14–BV786 (clone M5E2, BD Biosciences), anti-CD20–BV786 (clone L27,  
1185 BD Biosciences), anti-CD27–BUV395 (clone M-T271, BD Biosciences), anti-CD45RA–PE-Cy7  
1186 (clone 5H9, BD Biosciences), anti-CCR7–PE-Dazzle594 (clone G043H7, BioLegend), anti-  
1187 CXCR5–BV710 (clone RF8B2, BD Biosciences), and anti-TCF-1–PE (clone S33-966, BD  
1188 Biosciences). Data were acquired using an AriaIII flow cytometer (BD Biosciences) and  
1189 analyzed with FlowJo software version 10 (Tree Star Inc.).

1190

#### 1191 ***Measurement of SIV-suppressive activity***

1192 Autologous CD4<sup>+</sup> and CD8<sup>+</sup> T-cells were purified from freshly isolated PBMCs or tissue cell  
1193 suspensions by positive and negative selection, respectively, using the relevant EasySep Kits  
1194 with an automated RoboSep (StemCell Technologies). Purified CD4<sup>+</sup> T-cells were stimulated  
1195 for 3 days with concanavalin A (5µg/mL, Sigma-Aldrich) in the presence of IL-2 (100 IU/mL,  
1196 Miltenyi Biotec). Purified CD8<sup>+</sup> T-cells were cultured in the absence of mitogens and  
1197 cytokines (*ex vivo* CD8<sup>+</sup> T-cells). Stimulated CD4<sup>+</sup> T-cells (10<sup>5</sup>) were superinfected in U-  
1198 bottom 96-well plates with SIVmac251 (MOI = 10<sup>-3</sup>) in the presence (1:1 effector-to-target-  
1199 cell ratio) or absence of *ex vivo* CD8<sup>+</sup> T-cells (10<sup>5</sup>) from the same tissue via spinoculation for 1  
1200 hr (1,200 g at room temperature) and incubated for 1 hr at 37°C. Purified CD4<sup>+</sup> and CD8<sup>+</sup> T-  
1201 cells were separated in some assays using HTS Transwell-96 Permeable Supports with 0.4-  
1202 µm Pore Polycarbonate Membranes (Corning). Cells were then washed and cultured in R10

1203 medium containing IL-2 (100 IU/mL, Miltenyi Biotec). Culture supernatants were assayed on  
1204 day 7 using an SIV p27 Antigen ELISA Kit (Zeptometrix). Suppression of autologous virus was  
1205 assessed similarly without superinfection. Antiviral activity was calculated as  $\log_{10}$  (mean  
1206 p27 ng/mL in SIV-infected CD4<sup>+</sup> T-cell cultures without *ex vivo* CD8<sup>+</sup> T-cells) / (mean p27  
1207 ng/mL in SIV-infected CD4<sup>+</sup> T-cell cultures with *ex vivo* CD8<sup>+</sup> T-cells) (Saez-Cirion et al., 2010).

1208

#### 1209 **QUANTIFICATION AND STATISTICAL ANALYSIS**

1210 Data visualization was performed using Tableau version 2018.1.4 (Tableau Software).  
1211 Statistical analyses were performed using Prism version 8.1.2 (GraphPad Software) and  
1212 SigmaPlot version 12.5 (SYSTAT Software). Results are presented as median  $\pm$  IQR. Groups  
1213 were compared using the Mann-Whitney U-test. Correlations were assessed using Spearman  
1214 rank analyses. No adjustments were made for multiple comparisons, given the exploratory  
1215 nature of the analyses. All p values less than 0.05 were defined as significant.

1216

# Figure 1

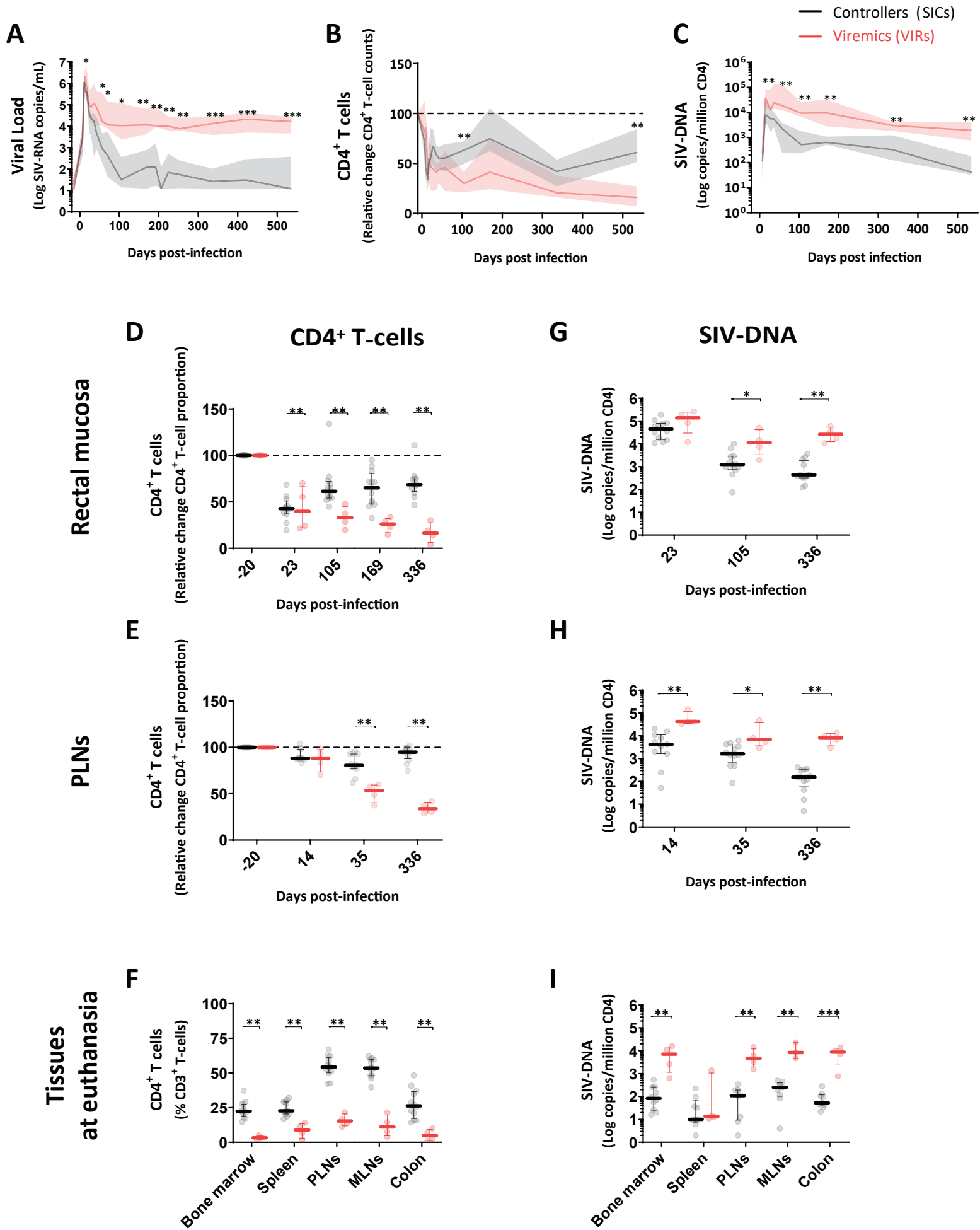
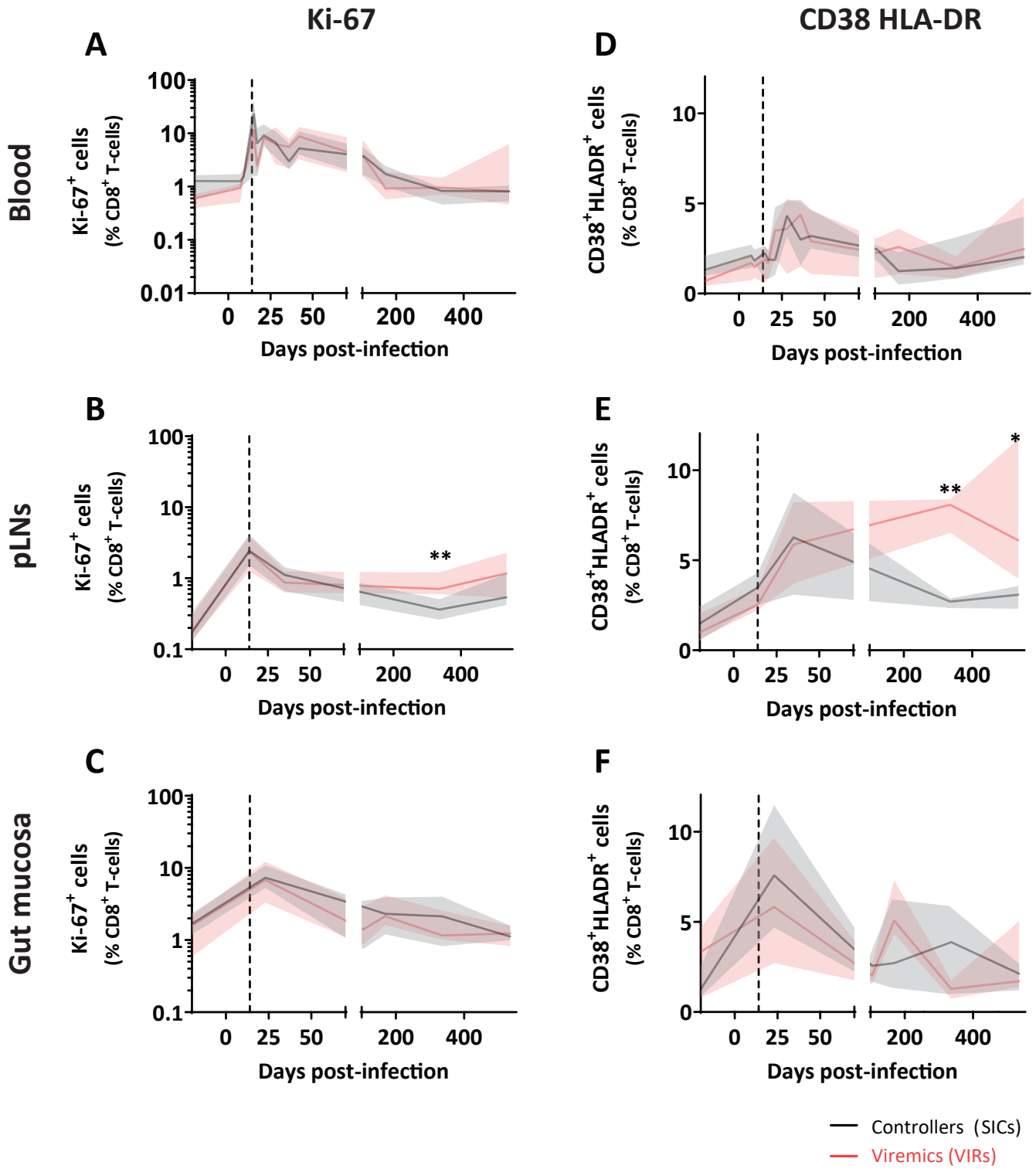
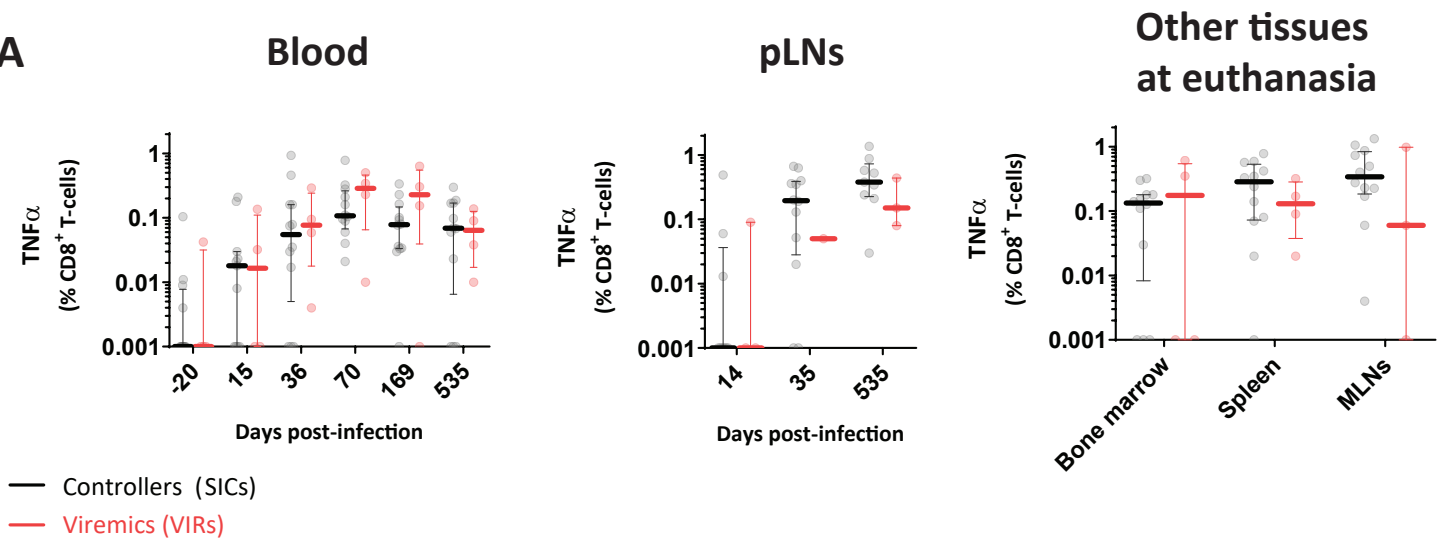


Figure 2



# Figure 3

## A



## B

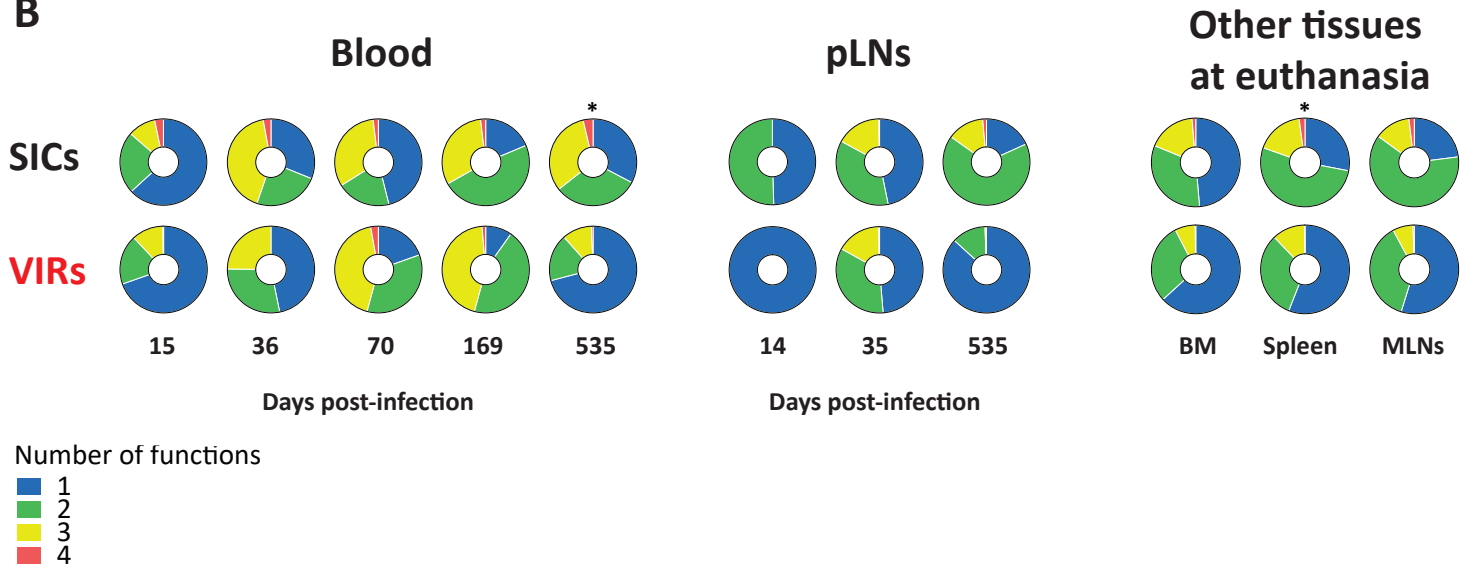


**Figure 4**

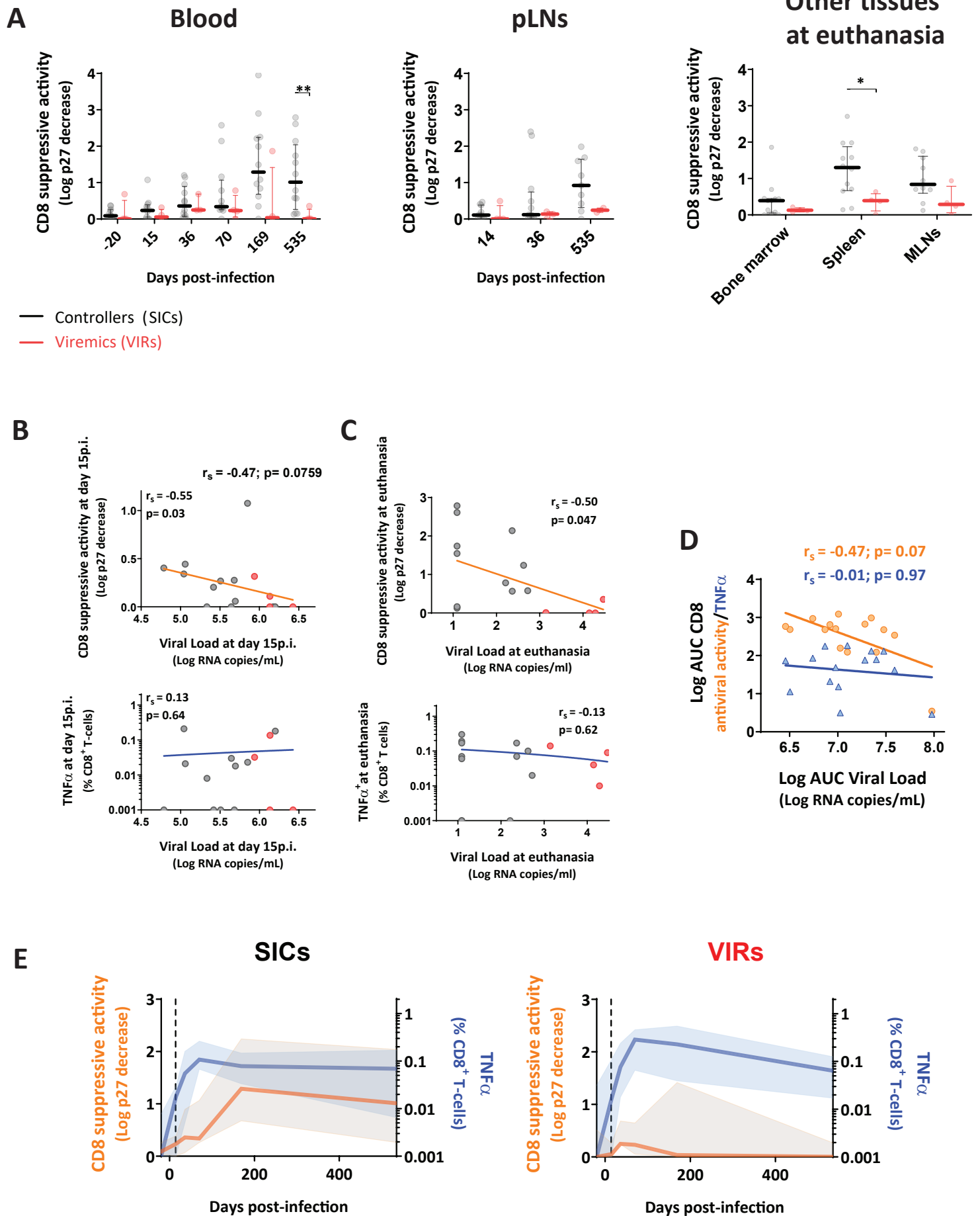


**Figure 5**

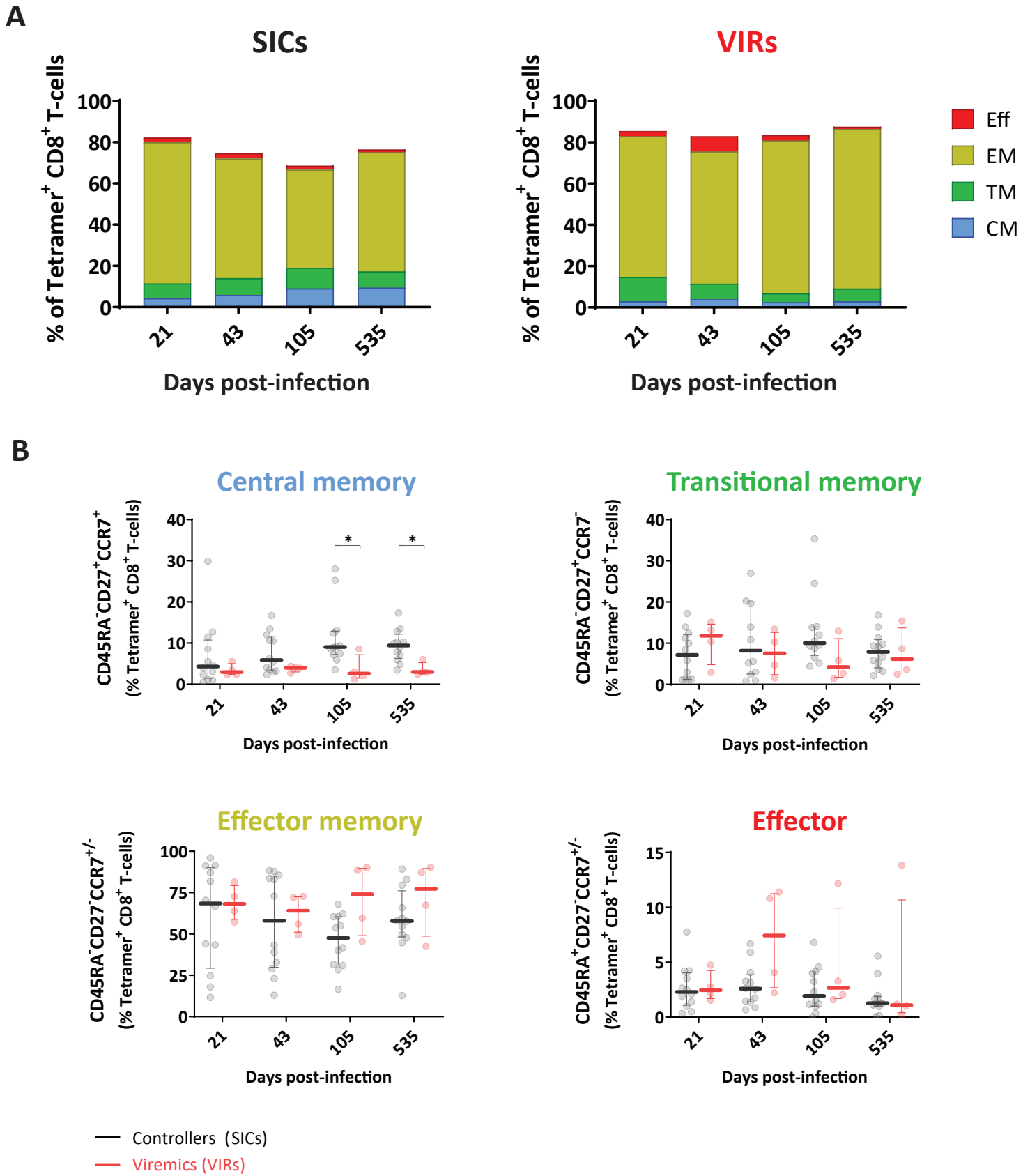
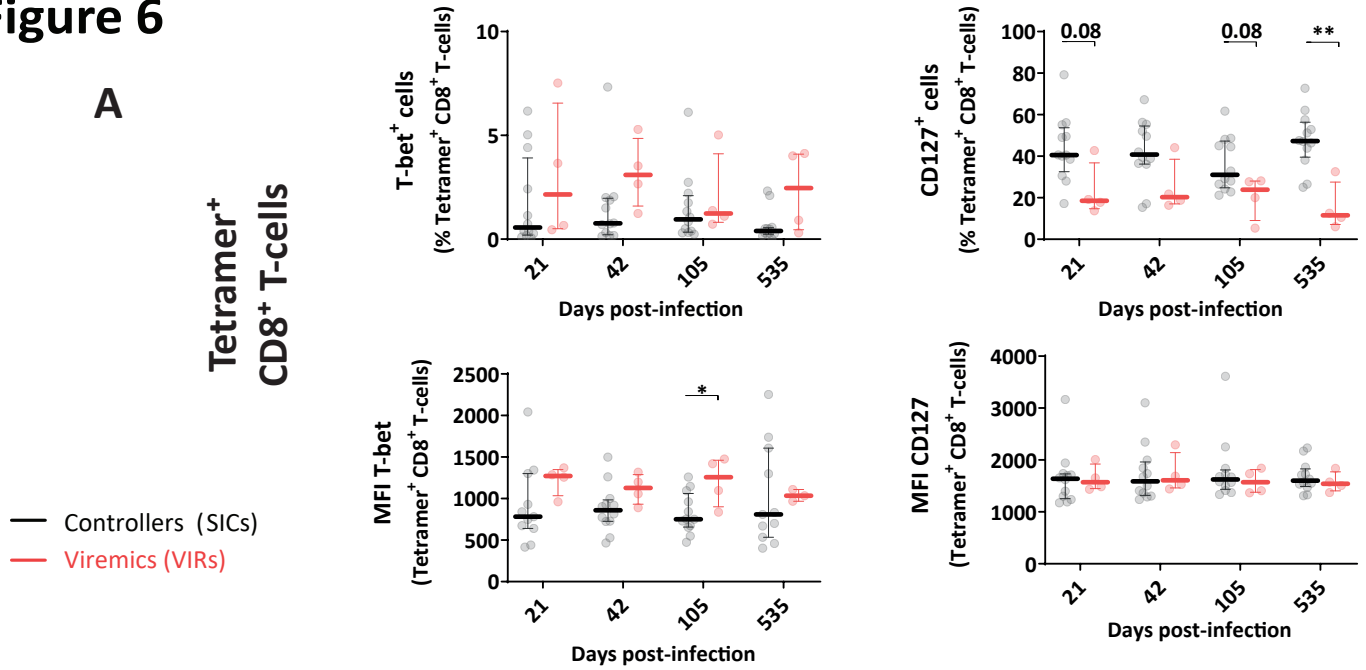


**Figure 6**

**A**



**B**

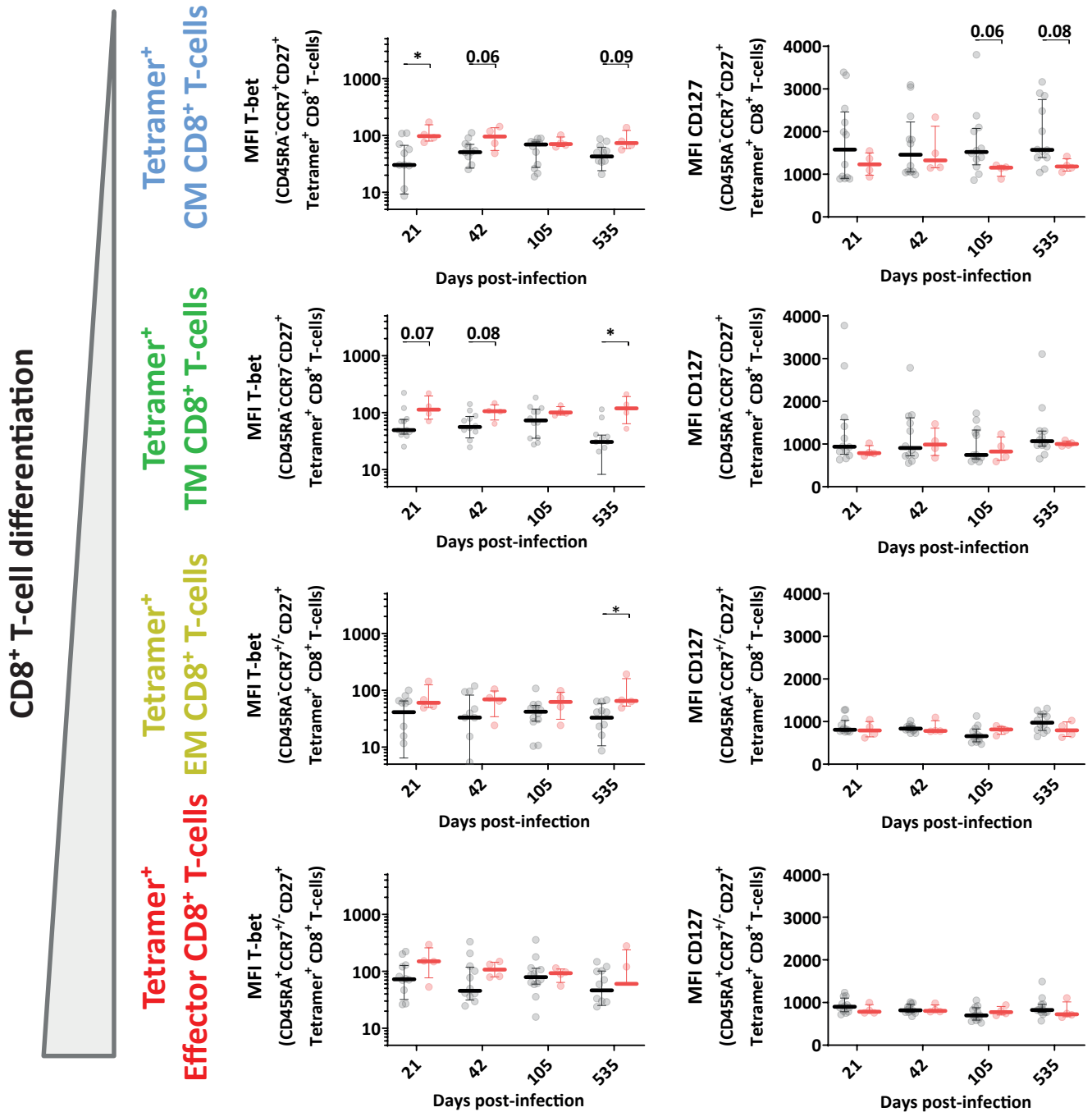
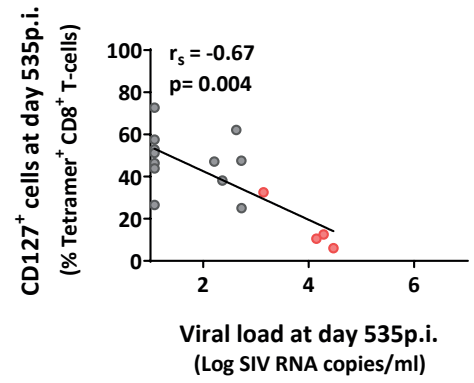
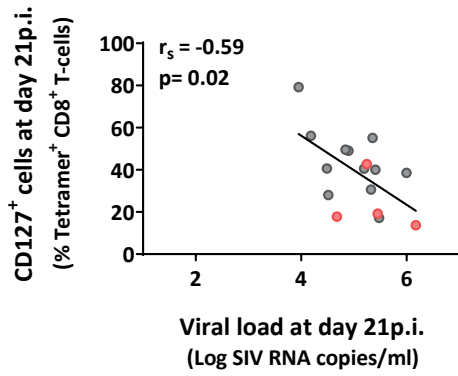
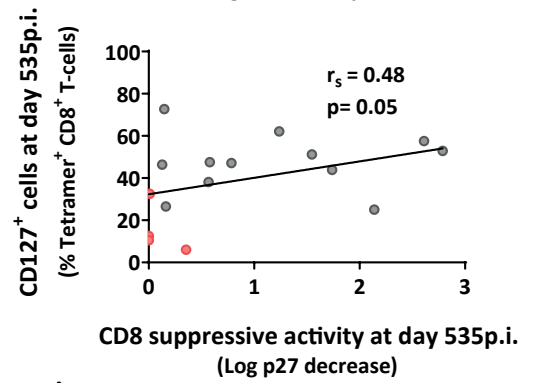
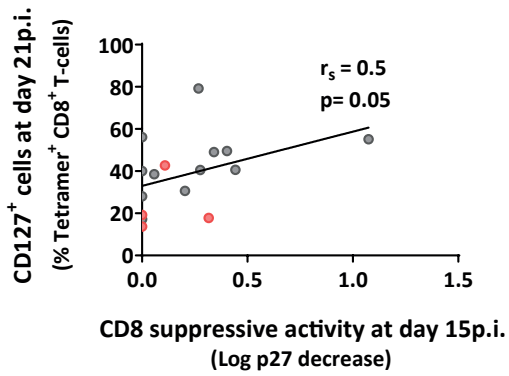


# Figure 7

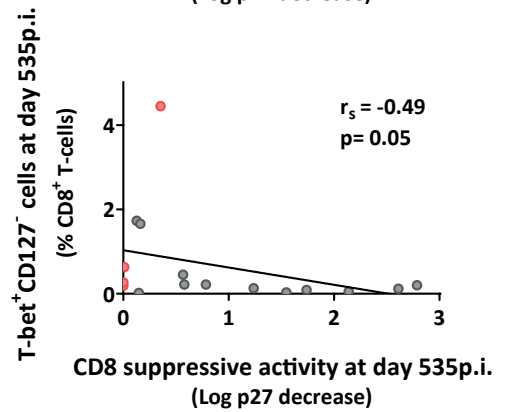
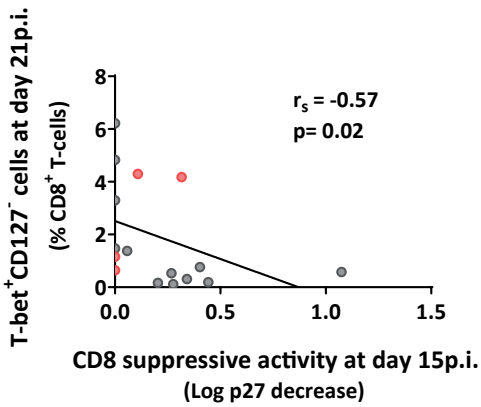
**A**



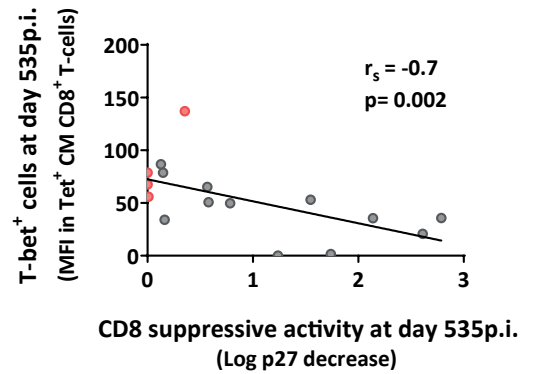
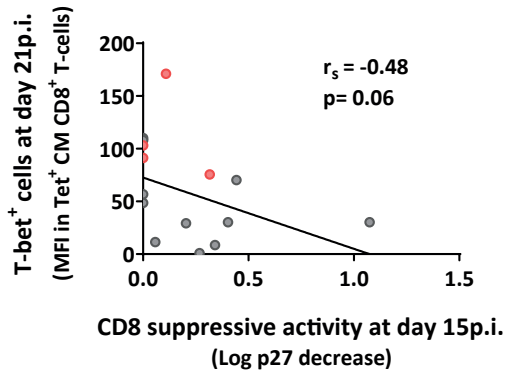
**B**



**C**



**D**



**E**

